

Optimizing stellarators for improved energetic particle stability and confinement

Elizabeth Paul

July 30, 2025

*... & my thoughts on AI/ML
for device design*

*Acknowledgements: A. Hyder, A. Knyazev, R. Jorge,
E. Rodriguez, D. Spong, H. Yoon*

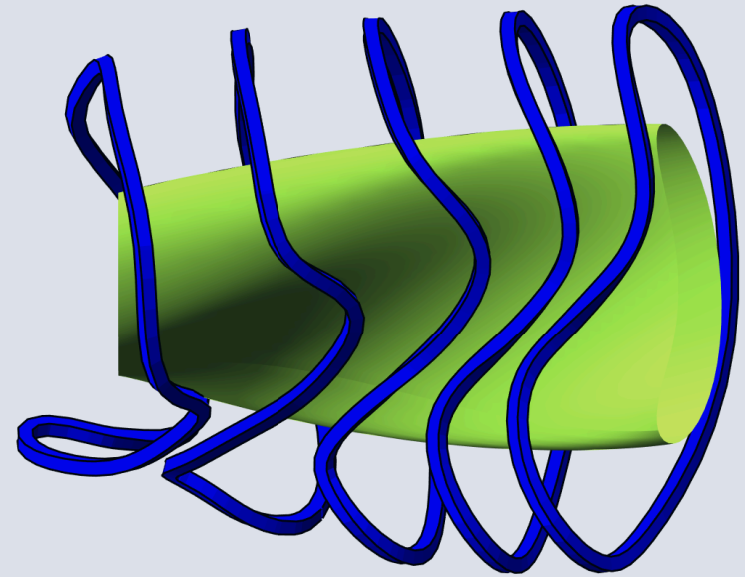
E. J. Paul et al, *J. Plasma Phys.*, 91 (2025). <https://doi.org/10.1017/S0022377825100524>

16th Plasma Kinetics Working Group Meeting



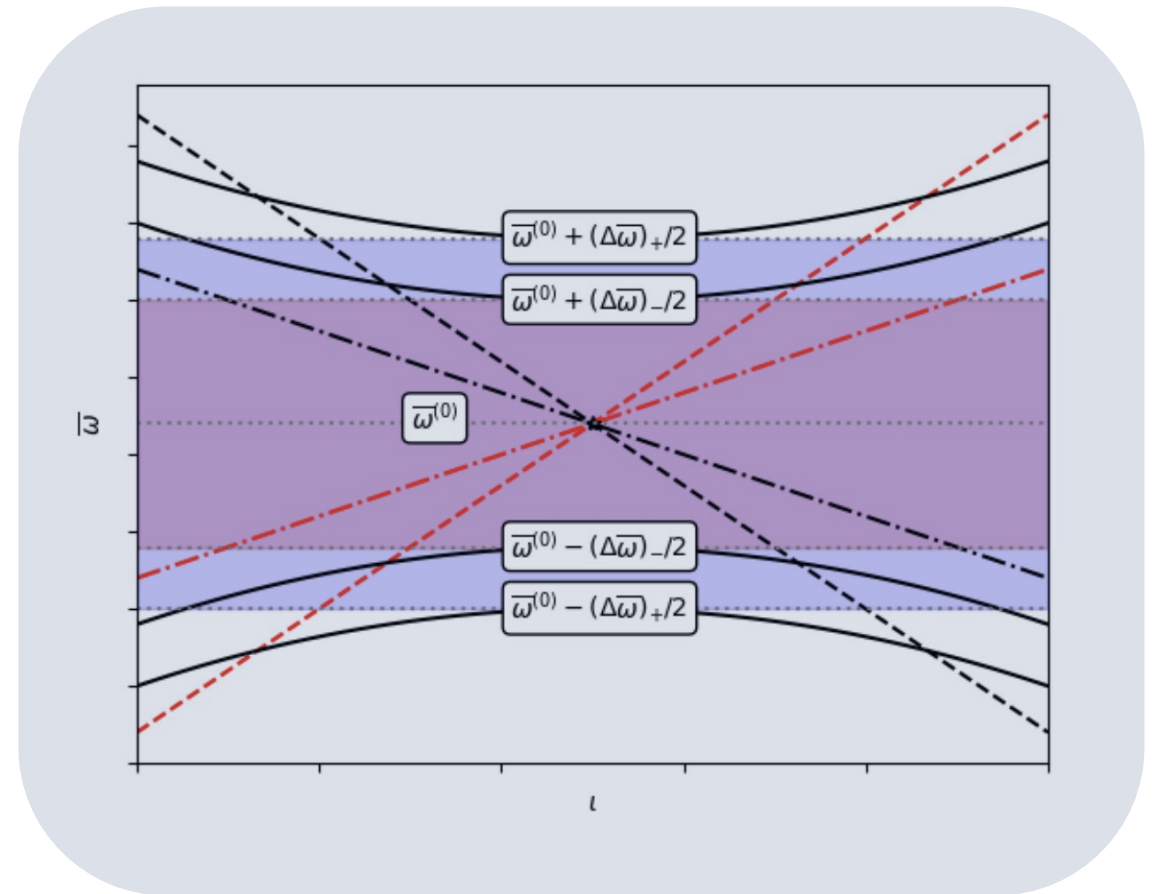
Outline

- *Stellarator optimization and AI/ML*
- *Perturbation theory for shear Alfvén continuum*
- *Can we manipulate the shear Alfvén continuum to avoid resonance?*



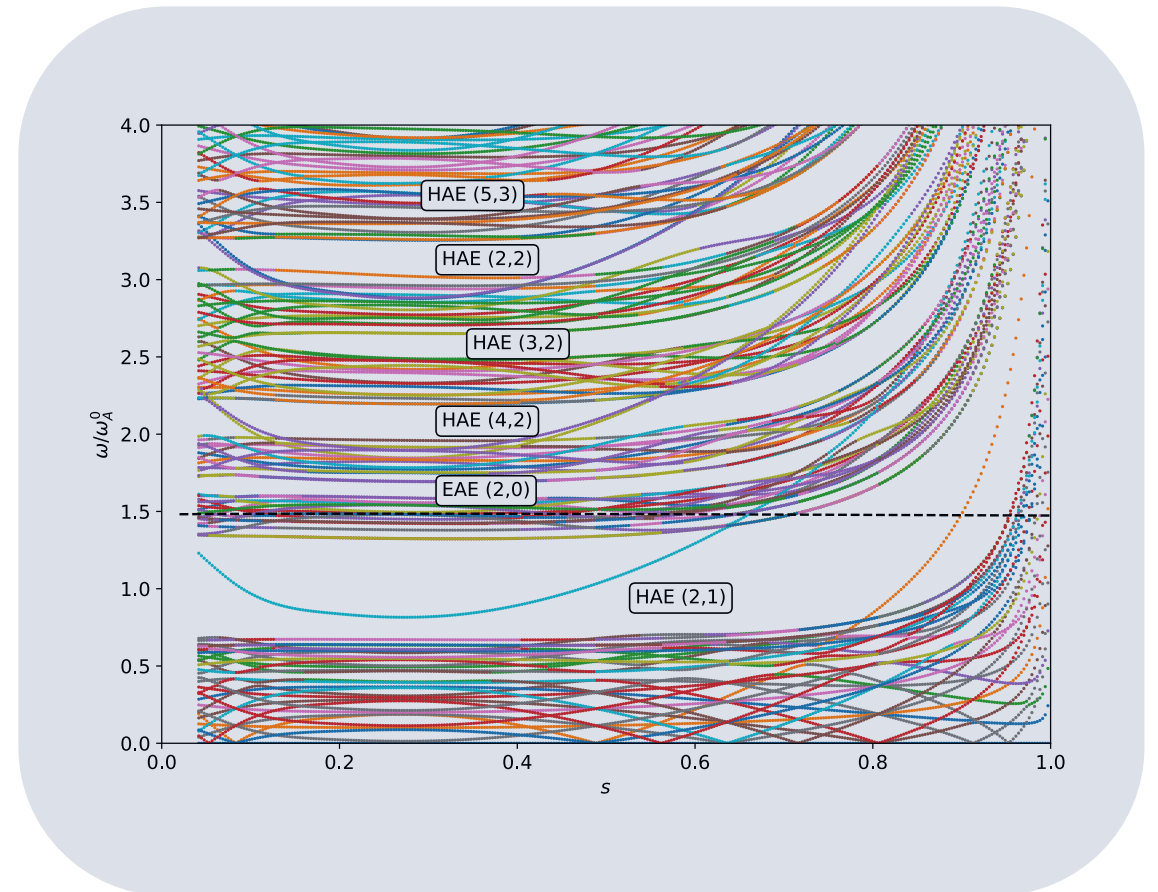
Outline

- *Stellarator optimization and AI/ML*
- ***Perturbation theory for shear Alfvén continuum***
- *Can we manipulate the shear Alfvén continuum to avoid resonance?*



Outline

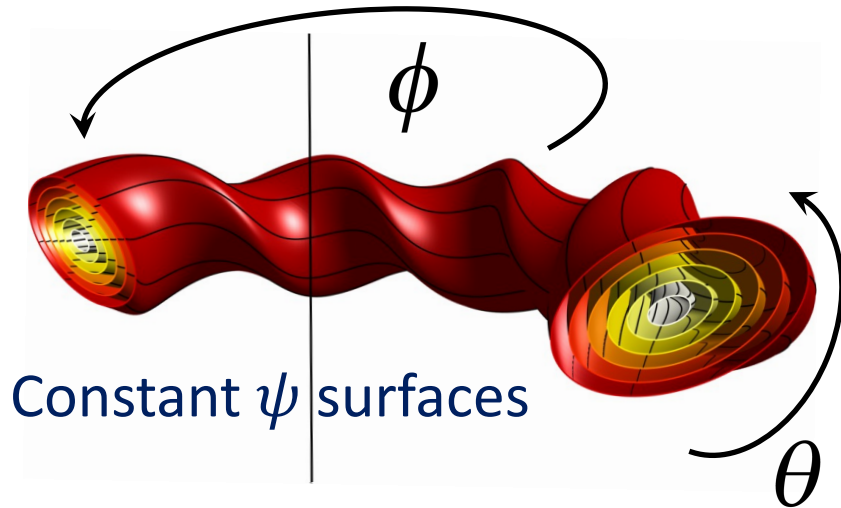
- *Stellarator optimization and AI/ML*
- *Perturbation theory for shear Alfvén continuum*
- ***Can we manipulate the shear Alfvén continuum to avoid resonance?***



$$\mathcal{L}(\mathbf{x}, \dot{\mathbf{x}}) = m \frac{|\dot{\mathbf{x}}|^2}{2} + q\mathbf{A}(\mathbf{x}) \cdot \dot{\mathbf{x}}$$

↓ Guiding center

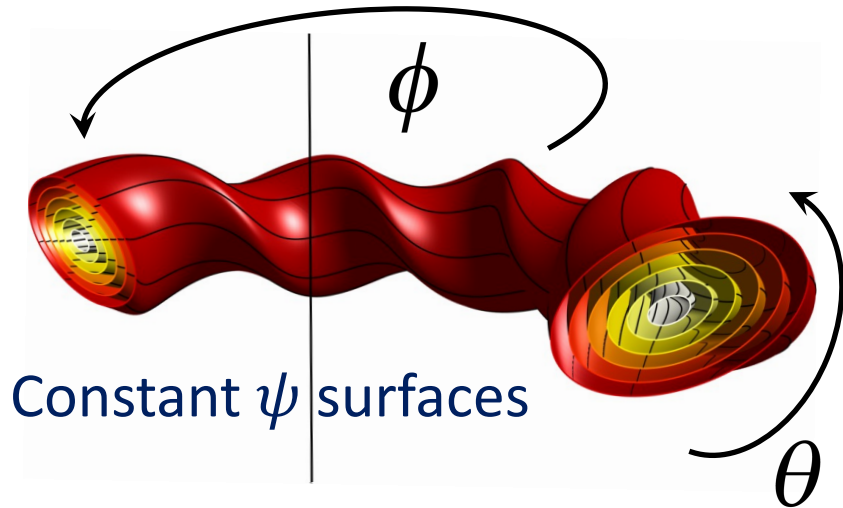
$$\mathcal{L}(\psi, \theta, \phi, \dot{\psi}, \dot{\theta}, \dot{\phi}) = \mathcal{L}(\psi, B(\psi, \theta, \phi), \dot{\psi}, \dot{\theta}, \dot{\phi})$$



$$\mathcal{L}(\mathbf{x}, \dot{\mathbf{x}}) = m \frac{|\dot{\mathbf{x}}|^2}{2} + q\mathbf{A}(\mathbf{x}) \cdot \dot{\mathbf{x}}$$

↓ Guiding center

$$\mathcal{L}(\psi, \theta, \phi, \dot{\psi}, \dot{\theta}, \dot{\phi}) = \mathcal{L}(\psi, B(\psi, \theta, \phi), \dot{\psi}, \dot{\theta}, \dot{\phi})$$



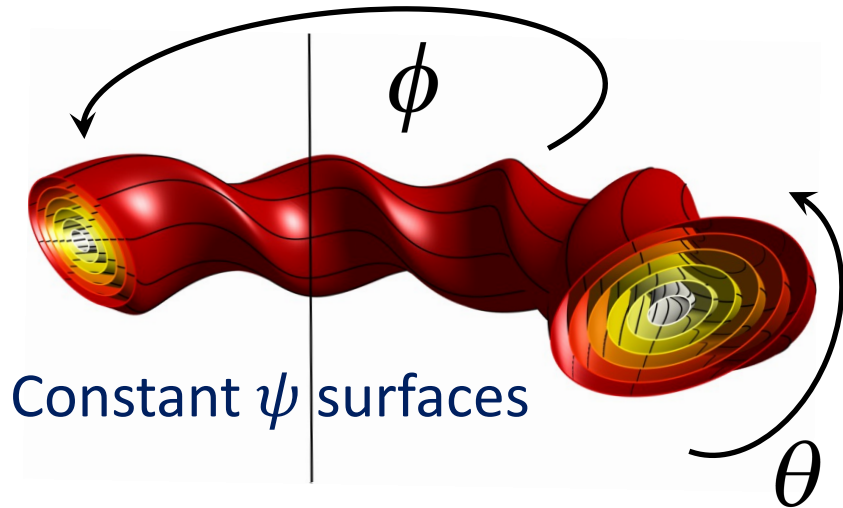
$$\frac{\partial B(\psi, \theta, \phi)}{\partial \phi} = 0 \longrightarrow \frac{dp_\phi}{dt} = 0$$

Ignorable coordinate **Conserved momentum**

$$\mathcal{L}(\mathbf{x}, \dot{\mathbf{x}}) = m \frac{|\dot{\mathbf{x}}|^2}{2} + q\mathbf{A}(\mathbf{x}) \cdot \dot{\mathbf{x}}$$

↓ **Guiding center**

$$\mathcal{L}(\psi, \theta, \phi, \dot{\psi}, \dot{\theta}, \dot{\phi}) = \mathcal{L}(\psi, B(\psi, \theta, \phi), \dot{\psi}, \dot{\theta}, \dot{\phi})$$



$$\frac{\partial B(\psi, \theta, \phi)}{\partial \phi} = 0 \longrightarrow \frac{dp_\phi}{dt} = 0$$

Ignorable coordinate **Conserved momentum**

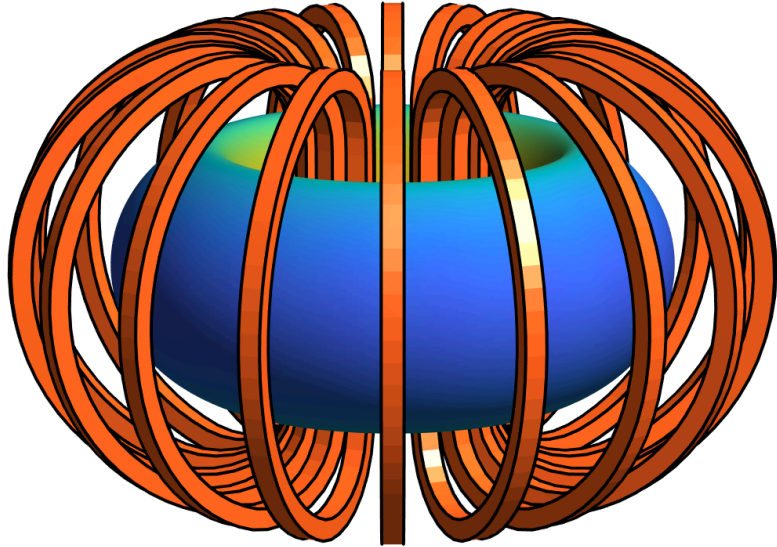
$$p_\phi = \cancel{\frac{mv_\phi}{qB}} + \underbrace{F(\psi)}$$

Particles stay confined to ψ surfaces

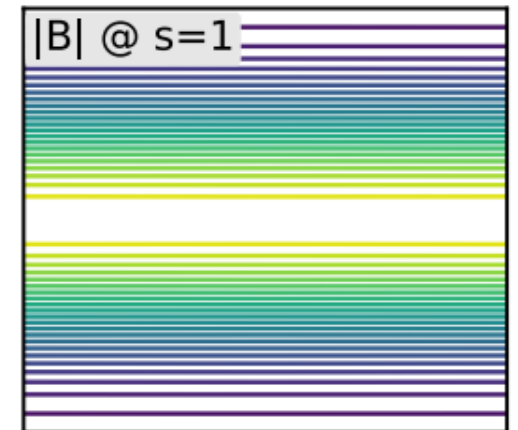
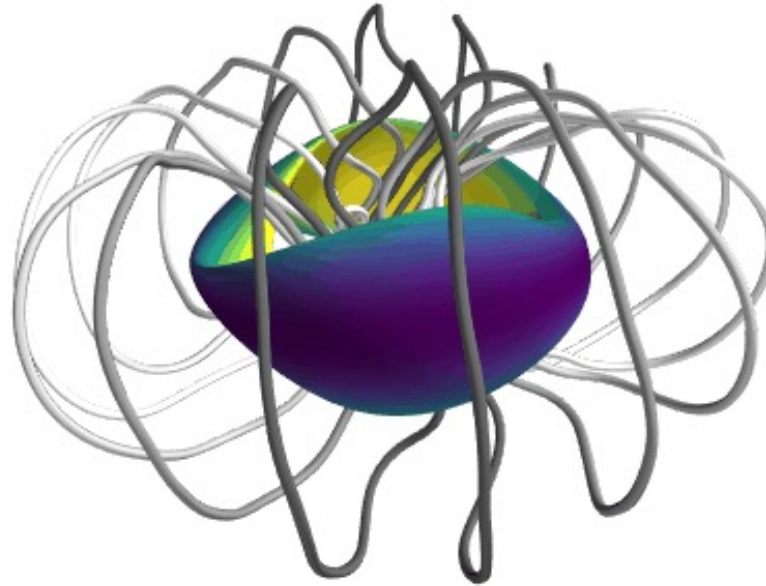
Quasisymmetry - a hidden symmetry of magnetic fields

2

Symmetric



Quasisymmetric



- ✓ Integrable magnetic field
- ✓ Energetic particle confinement
- ✓ MHD stability
- ✓ Collisional “bootstrap” current
- ✓ Equilibrium β limit
- ✓ Divertor configuration
- ✓ Reduction of turbulent transport
- ✓ **Coil feasibility**



ASG Superconductors

1. MHD equilibrium optimization

*Boundary of equilibrium
optimized for confinement*

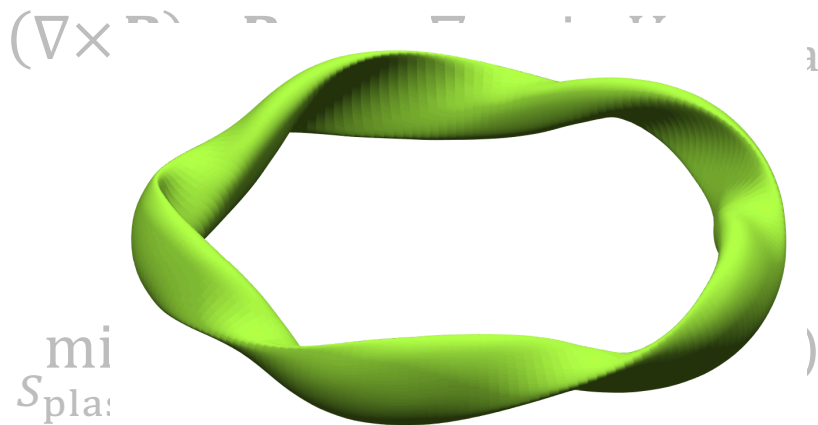
$$(\nabla \times \mathbf{B}) \times \mathbf{B} = \mu_0 \nabla p \quad \text{in } V_{\text{plasma}}$$

$$\mathbf{B} \cdot \hat{\mathbf{n}} \Big|_{S_{\text{plasma}}} = 0$$

$$\min_{S_{\text{plasma}}} f(\mathbf{B}(S_{\text{plasma}}), S_{\text{plasma}})$$

1. MHD equilibrium optimization

*Boundary of equilibrium
optimized for confinement*



2. Coil design

*Inverse problem solved to find coils
to support equilibrium*

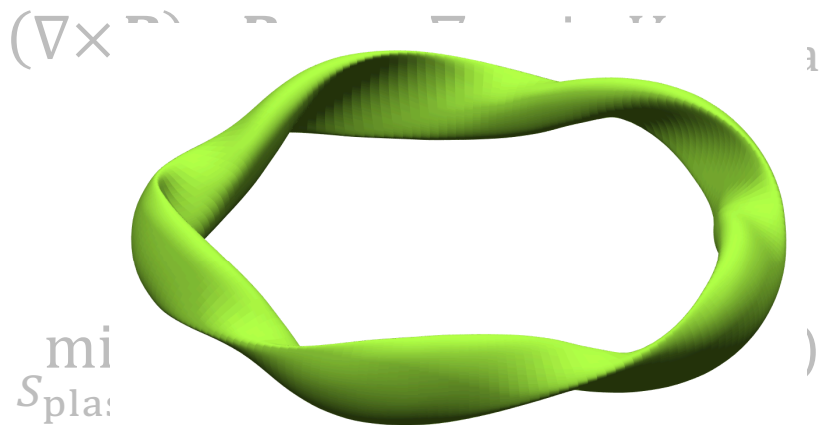
$$\begin{aligned}
 \mathbf{B} \cdot \hat{\mathbf{n}} &= \mathbf{B}_{\text{plasma}} \cdot \hat{\mathbf{n}} \\
 &+ \frac{\mu_0}{4\pi} \int_{\mathbb{R}^3 \setminus V_{\text{plasma}}} d^3x' \frac{\mathbf{J}_{\text{coil}}(\mathbf{x}') \times (\mathbf{x} - \mathbf{x}') \cdot \hat{\mathbf{n}}(\mathbf{x})}{|\mathbf{x} - \mathbf{x}'|^3}
 \end{aligned}$$

$$\min_{J_{\text{coil}}} \left(\int_{S_{\text{plasma}}} d^2x (\mathbf{B} \cdot \hat{\mathbf{n}})^2 + (\text{coil complexity}) \right)$$

Traditional two-step optimization

1. MHD equilibrium optimization

*Boundary of equilibrium
optimized for confinement*



2. Coil design

*Inverse problem solved to find coils
to support equilibrium*

$$B \cdot \hat{n} = B_{\text{plasma}} + \frac{\mu_0}{4\pi} \int_{\mathbb{R}^3} \frac{(x-x') \cdot \hat{n}(x)}{|x-x'|^3} dV'$$

$$\min_{J_{\text{coil}}} \left(\int_{S_{\text{plasma}}} dS \left(\frac{1}{R} + \text{complexity} \right) \right)$$

A 3D visualization of a toroidal plasma equilibrium boundary (green) surrounded by a blue magnetic coil structure.

nature

Article

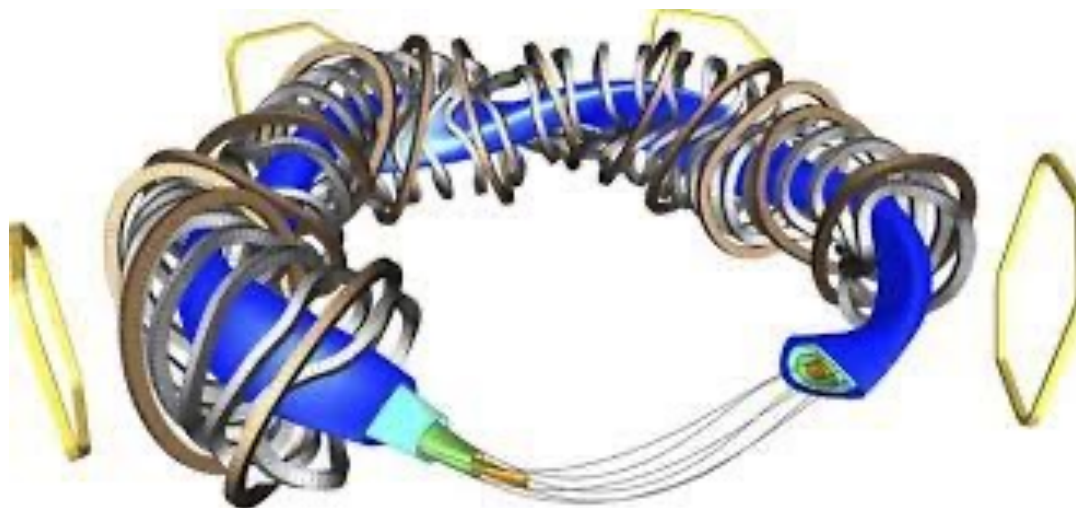
Demonstration of reduced neoclassical energy transport in Wendelstein 7-X

<https://doi.org/10.1038/s41586-021-03687-w>

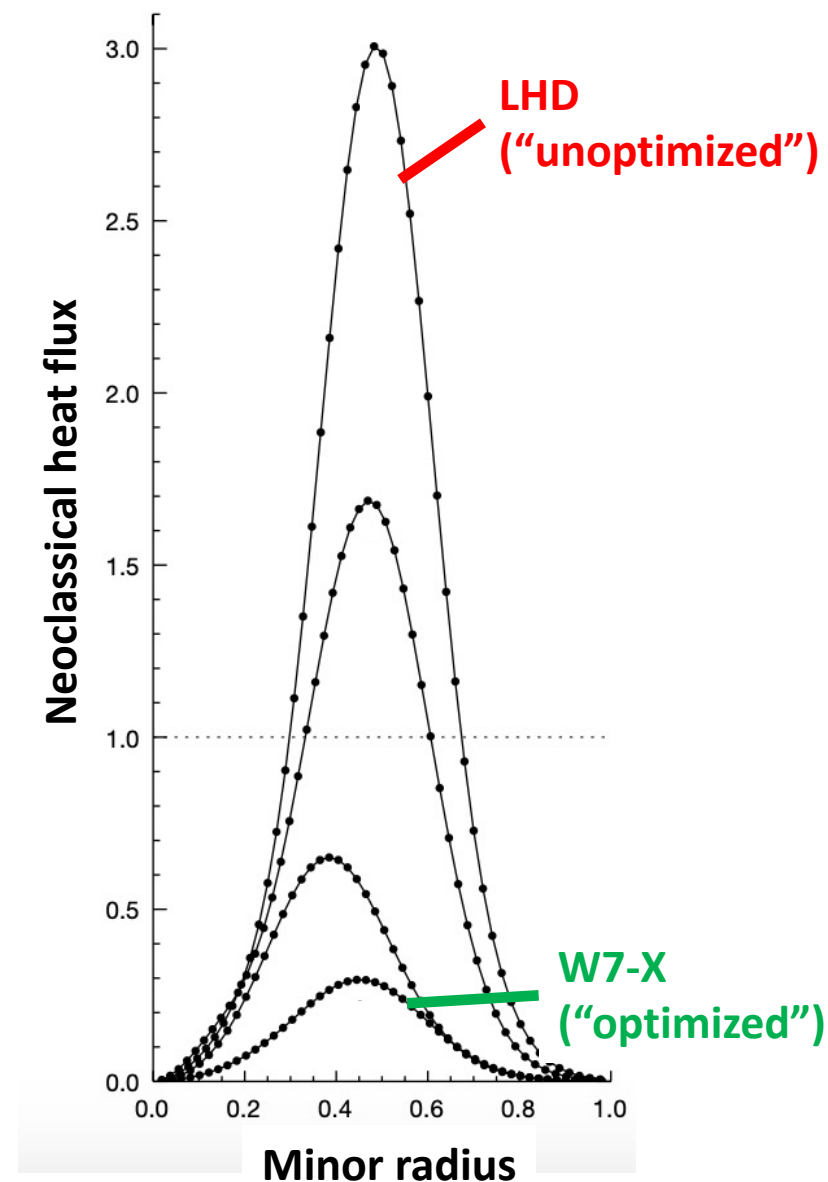
Received: 30 April 2020

Accepted: 2 June 2021

Published online: 11 August 2021



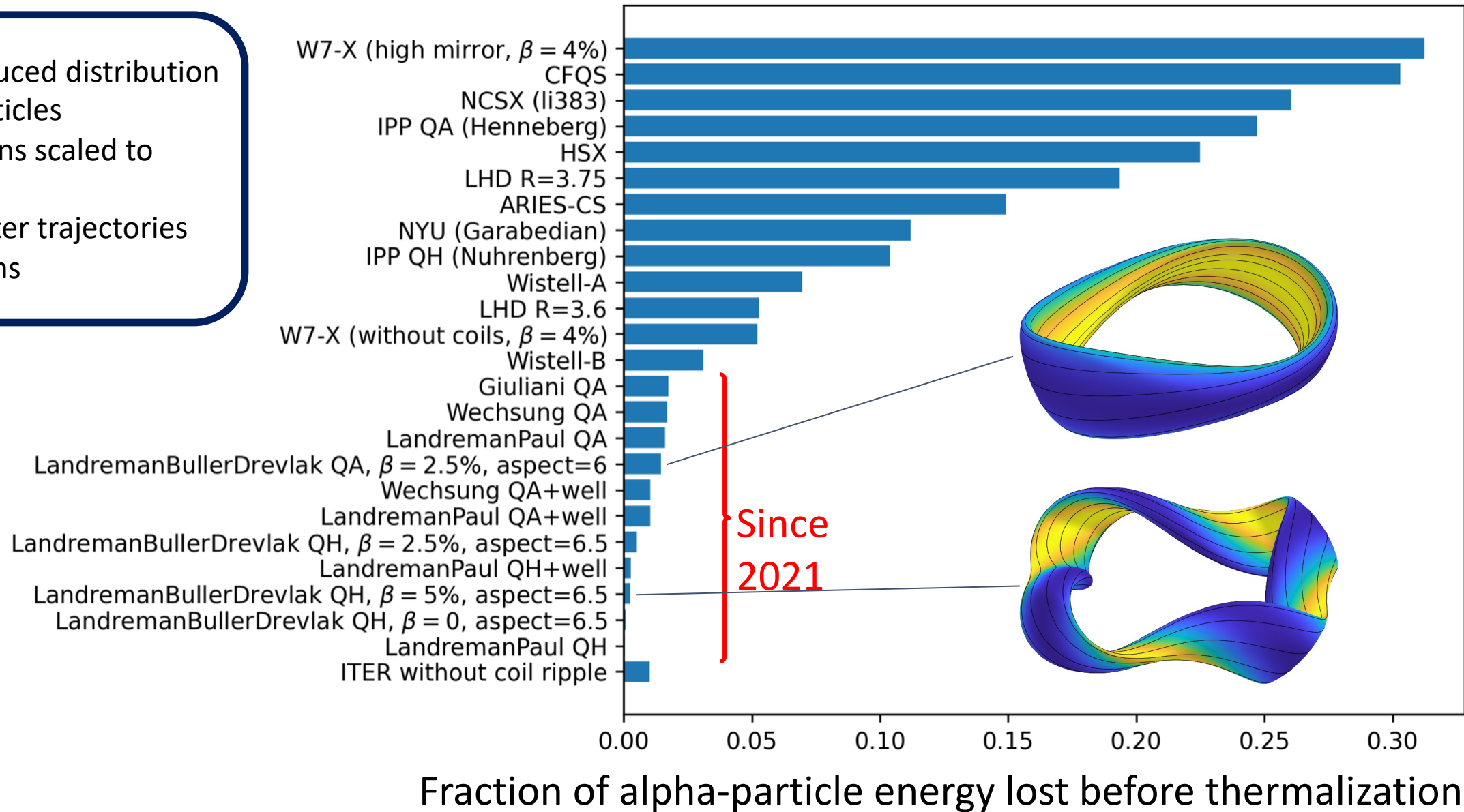
C. D. Beidler¹✉, H. M. Smith¹, A. Alonso², T. Andreeva¹, J. Baldzuhn¹, M. N. A. Beurskens¹, M. Borchardt¹, S. A. Bozhakov¹, K. J. Brunner¹, H. Damm¹, M. Drevlak¹, O. P. Ford¹, G. Fuchert¹, J. Geiger¹, P. Helander¹, U. Hergenroth^{1,5}, M. Hirsch¹, U. Höfel¹, Ye. O. Kazakov³, R. Kleiber¹, M. Krychowiak¹, S. Kwak¹, A. Langenberg¹, H. P. Laqua¹, U. Neuner¹, N. A. Pablant⁴, E. Pasch¹, A. Pavone¹, T. S. Pedersen¹, K. Rahbarnia¹, J. Schilling¹, E. R. Scott¹, T. Stange¹, J. Svensson¹, H. Thomsen¹, Y. Turkin¹, F. Warmer¹, R. C. Wolf¹, D. Zhang¹ & the W7-X Team*

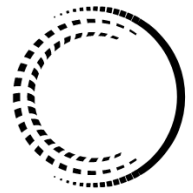


Through optimization, QS stellarators can confine fusion products

6

- Fusion-produced distribution of alpha particles
- Configurations scaled to reactor size
- Guiding center trajectories with collisions





THEA ENERGY

TYPE ONE
ENERGY



STELLAREX



RENAISSANCE
FUSION



GAUSS
FUSION


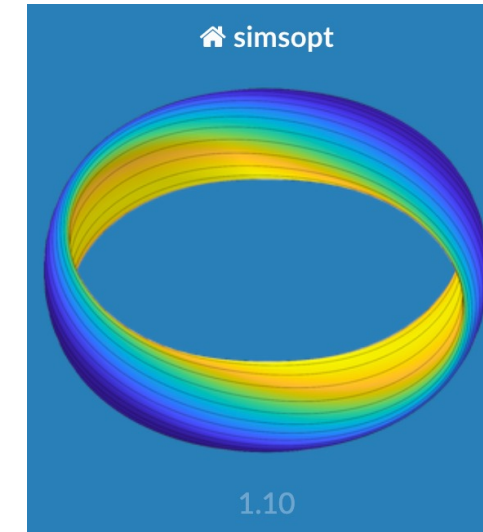


Proxima
Fusion



Helical
Fusion

- Automatic differentiation (JAX)
 - ✗ Software must be rewritten with JAX-compatible functions
 - ✗ Potential poor memory scaling (intermediate values stored)
 - ✓ (relatively) straightforward to implement new objectives



Stellarator Optimization Package

license MIT DOI 10.5281/zenodo.4876504 issues 180 open pypi v0.14.2


docs passing Unit tests passing Regression tests passing codecov 95%

DESC solves for and optimizes 3D MHD equilibria using pseudo-spectral numerical methods and automatic differentiation.

monkes

Monoenergetic Kinetic Equation Solver

This is a python/JAX port of the [original fortran implementation](#). It solves the drift kinetic equation (DKE) using the monoenergetic approximation, similar to DKES, but uses JAX so it runs on GPUs and is differentiable.



ESSOS

ESSOS: e-Stellarator Simulation and Optimization Suite

license MIT last commit july python 100.0% Build and Test passing codecov 31% docs passing

- Automatic differentiation (JAX)
 - ✗ Software must be rewritten with JAX-compatible functions
 - ✗ Potential poor memory scaling (intermediate values stored)
 - ✓ (relatively) straightforward to implement new objectives

```
@jit
def curve_length_pure(l):
    """
    Compute the mean of the incremental arclengths along a curve (the curve length).

    Args:
        l (array-like): Array of incremental arclengths along the curve.

    Returns:
        float: The mean arclength (i.e., the curve length).
    """
    return jnp.mean(l)
```

```
class CurveLength(Optimizable):
    """
    CurveLength is a class that computes the length of a curve, i.e.

    .. math::
        J = \int_{\text{curve}} dl.

    """

    def __init__(self, curve):
        self.curve = curve
        self.dJ_dL = jit(lambda l: grad(curve_length_pure)(l))
        super().__init__(depends_on=[curve])

    def J(self):
        """
        This returns the value of the quantity.
        """
        return curve_length_pure(self.curve.incremental_arclength())

    @derivative_dec
    def dJ(self):
        """
        This returns the derivative of the quantity with respect to the curve dofs.
        """

        return self.curve.dincremental_arclength_by_dcoeff_vjp(
            self.dJ_dL(self.curve.incremental_arclength()))

    return_fn_map = {'J': J, 'dJ': dJ}
```

- Automatic differentiation (JAX)

- ✗ Software must be rewritten with JAX-compatible functions
- ✗ Potential poor memory scaling (intermediate values stored)
- ✓ (relatively) straightforward to implement new objectives

- Adjoint methods

- Enforce constraint with Lagrange multiplier:

$$\mathcal{L}(\Omega, u, q) = f(\Omega, u) + \langle q, L(\Omega, u) \rangle$$

- Solve *adjoint* equation:

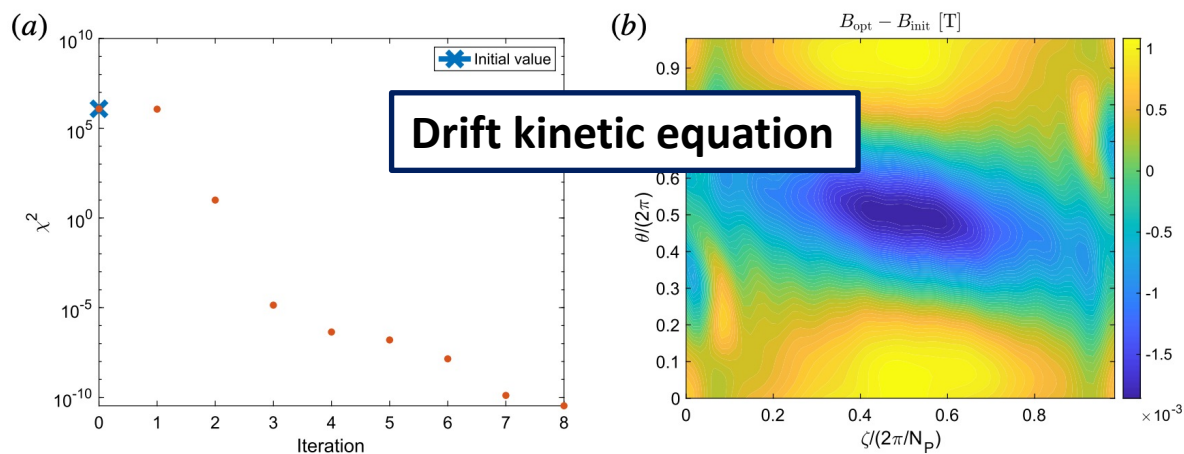
$$\delta \mathcal{L}(\Omega, u, q; \delta u) = 0$$

- Compute derivative of cost function

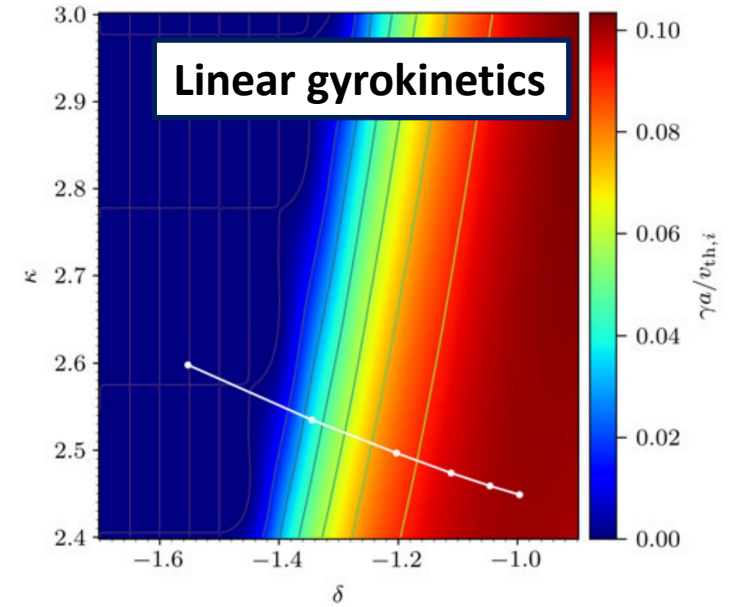
$$\delta f(\Omega, u(\Omega), q; \delta \Omega) = \delta \mathcal{L}(\Omega, u(\Omega), q; \delta \Omega)$$

- u = state variables
- Ω = design parameters
- q = test function
- f = cost function
- $\langle \dots \rangle$ = inner product

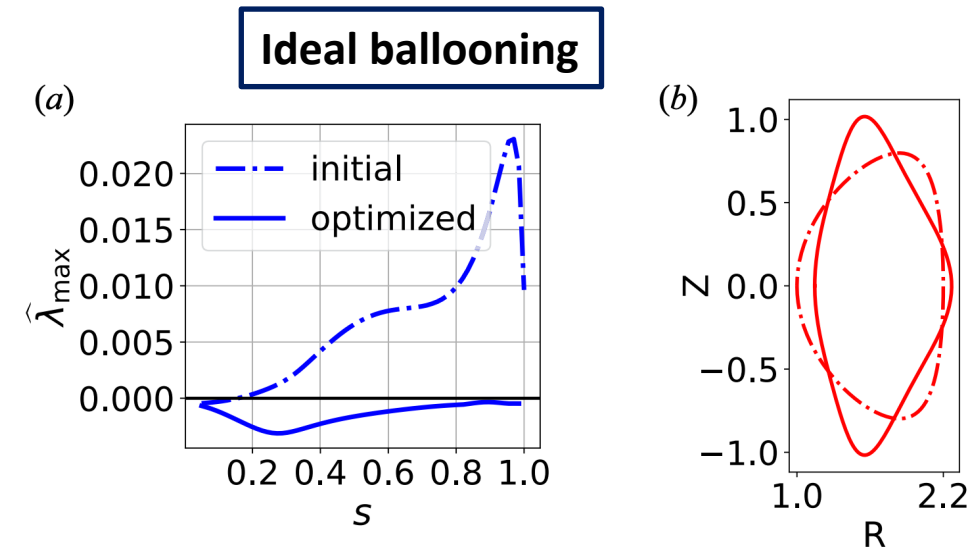
- Automatic differentiation (JAX)
 - ✗ Software must be rewritten with JAX-compatible functions
 - ✗ Potential poor memory scaling (intermediate values stored)
 - ✓ (relatively) straightforward to implement new objectives
- Adjoint methods
 - ✗ Requires deriving new equations for new objectives
 - ✓ Reduction in memory overhead and computational cost (if # objectives \ll # parameters)
 - ✓ Legacy solvers can be reused (with modifications)



Paul et al, *J. Plasma Phys.* 85 (2019).



Acton et al, *J. Plasma Phys.* 90 (2024).



Gaur et al, *J. Plasma Phys.* 89 (2023).

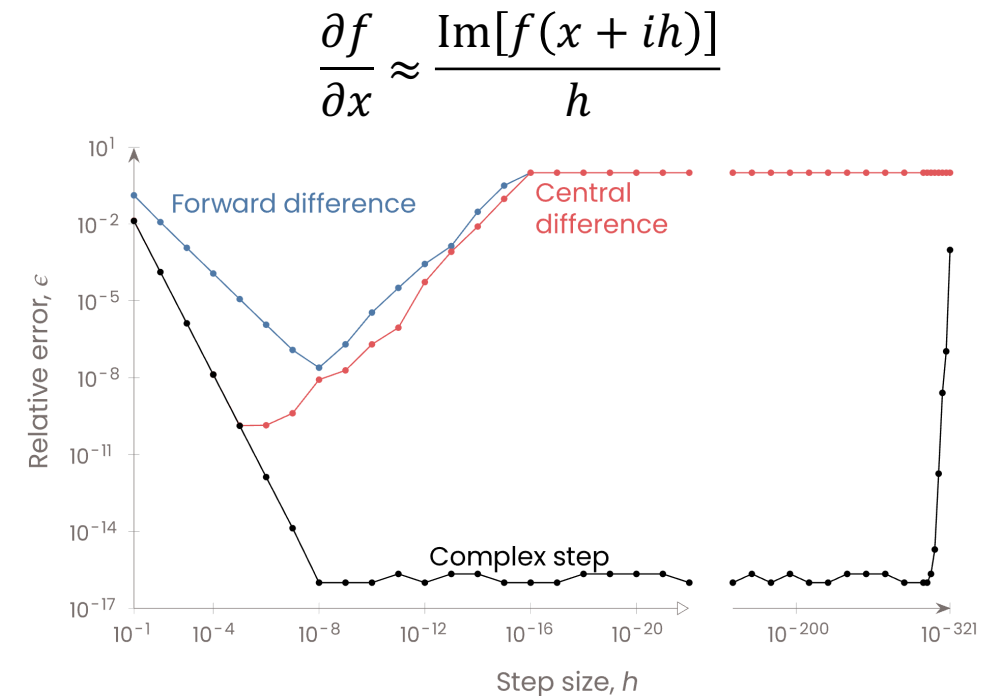
- Automatic differentiation (JAX)
 - ✗ Software must be rewritten with JAX-compatible functions
 - ✗ Potential poor memory scaling (intermediate values stored)
 - ✓ (relatively) straightforward to implement new objectives

- Adjoint methods

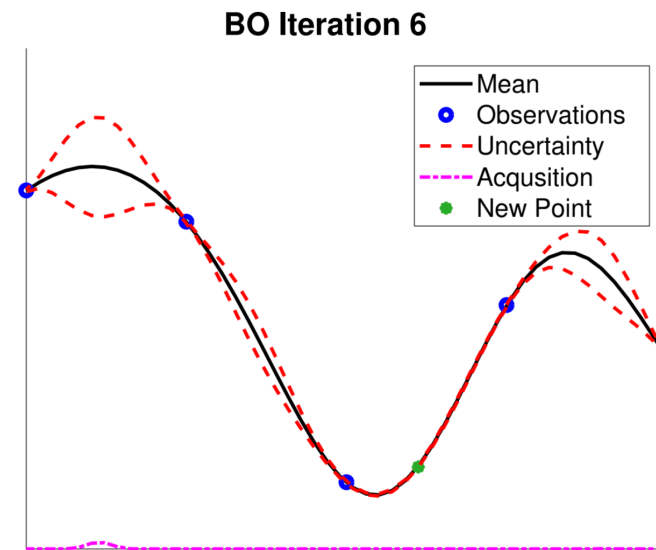
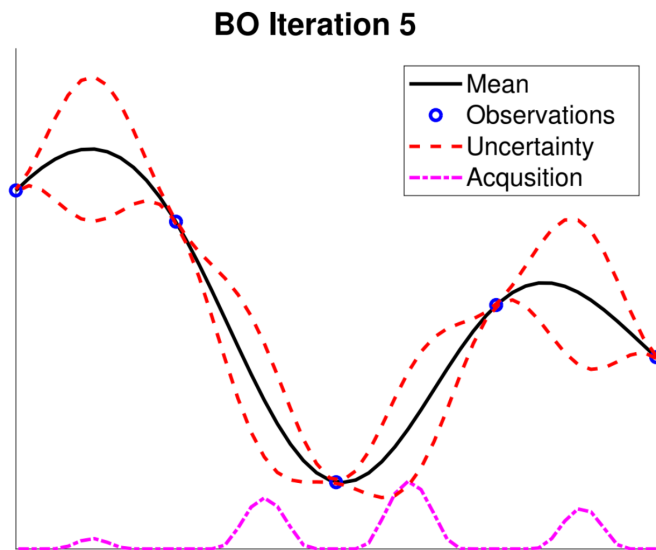
- ✗ Requires deriving new equations for new objectives
 - ✓ Reduction in memory overhead and computational cost (if # objectives \ll # parameters)
 - ✓ Legacy solvers can be reused (with modifications)

- Complex step differentiation

- ✗ Requires complex analytic function
 - ✗ Expensive for high-dimensional gradient
 - ✓ Simple implementation



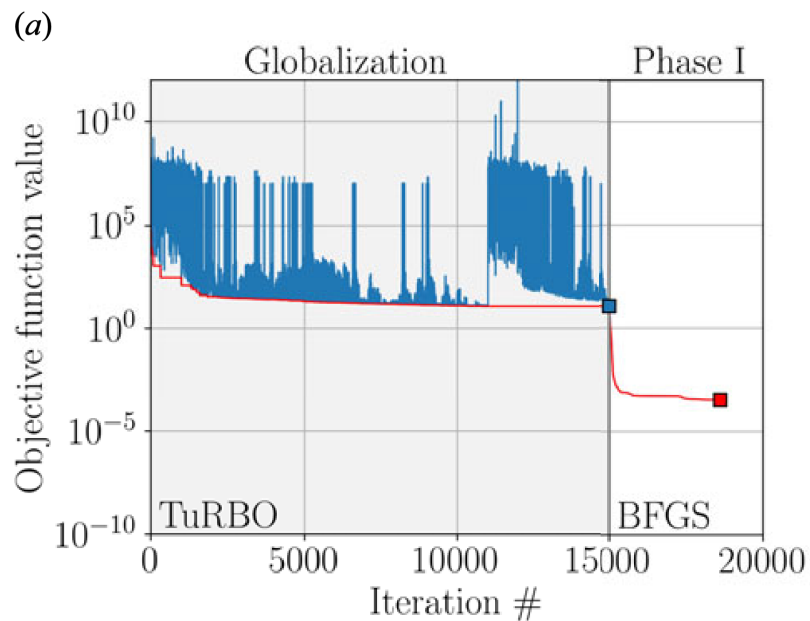
- Optimizing with data-driven surrogate models
 - **Bayesian optimization:**
 - Build Gaussian process surrogate based on limited function evaluations
 - Challenge: scaling to many ($\gtrsim 20$) dimensions often impractical
 - Incorporating gradients, several local BOs can help [Padidar, NeurIPS 2021]



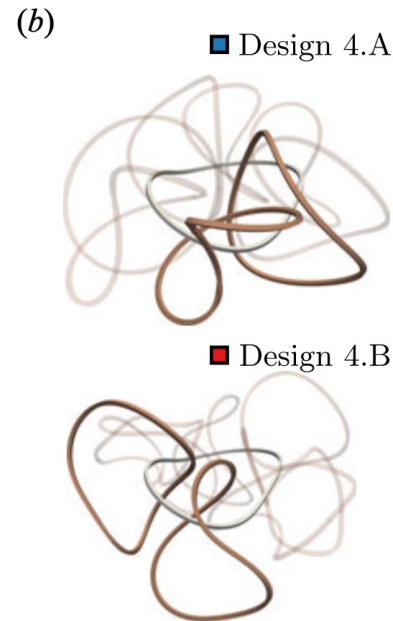
How can data-driven methods accelerate device optimization?

- Optimizing with data-driven surrogate models
 - Bayesian optimization:**
 - Build Gaussian process surrogate based on limited function evaluations
 - Challenge: scaling to many ($\gtrsim 20$) dimensions often impractical
 - Incorporating gradients, several local BOs can help [Padidar, NeurIPS 2021]

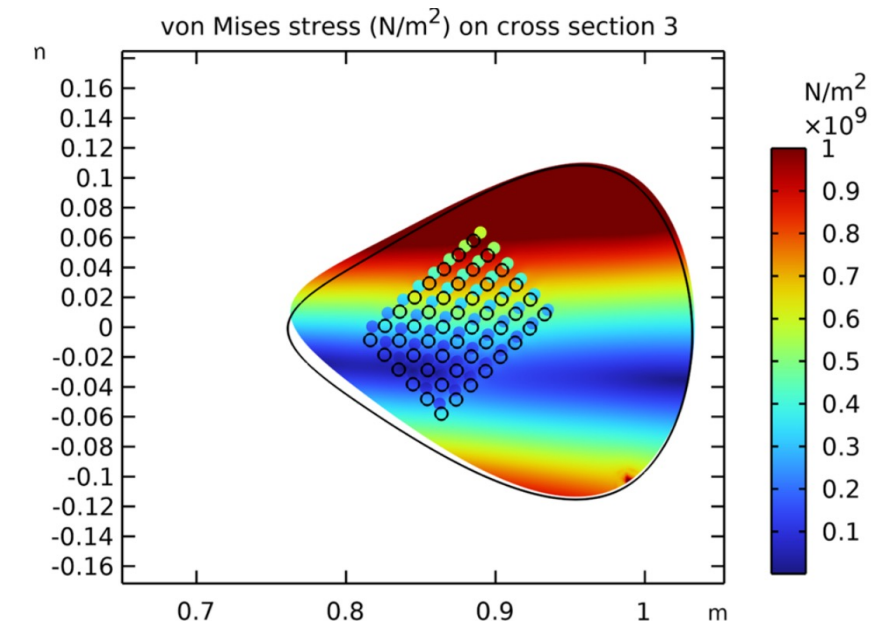
Initial stage coil exploration



Giuliani et al, *J. Plasma Phys.* 90 (2024).

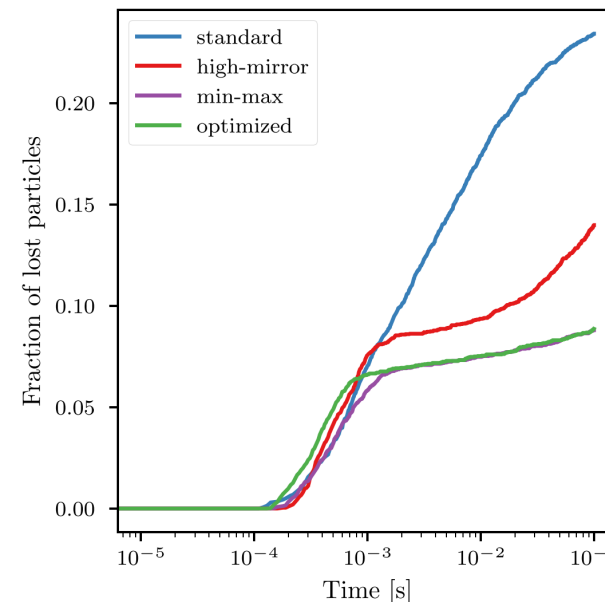
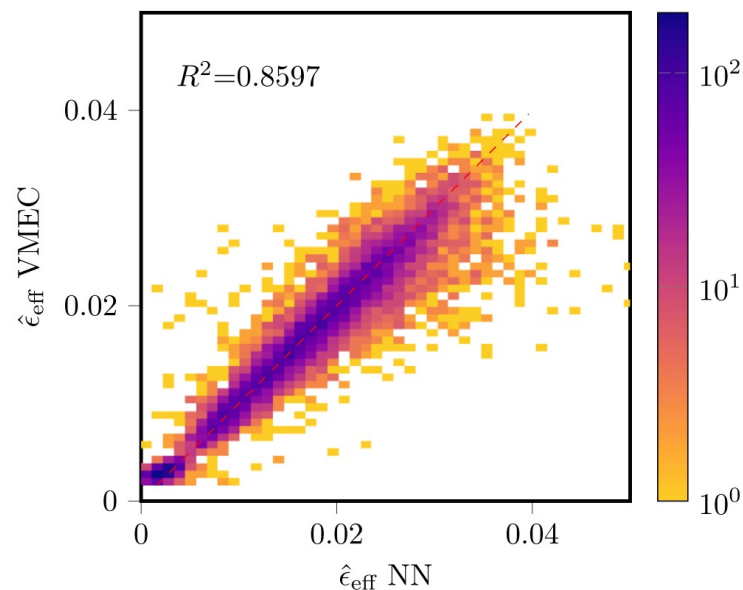


Coil winding pack optimization



Packman et al, *J. Fusion Energy* 44 (2025).

- Optimizing with data-driven surrogate models
 - **Bayesian optimization:**
 - Build Gaussian process surrogate based on limited function evaluations
 - Challenge: scaling to many ($\gtrsim 20$) dimensions often impractical
 - Incorporating gradients, several local BOs can help [Padidar, NeurIPS 2021]
 - **Neural network surrogates:**
 - Provides differentiable model
 - Likely only feasible within a limited configuration space (e.g., W7-X operating space)

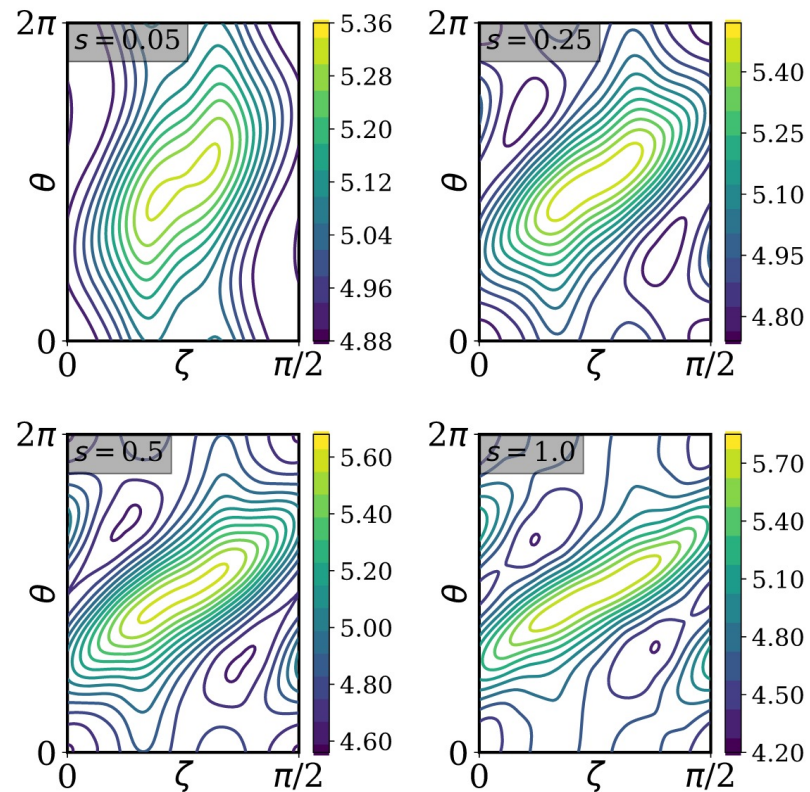


- Optimizing with data-driven surrogate models
 - **Bayesian optimization:**
 - Build Gaussian process surrogate based on limited function evaluations
 - Challenge: scaling to many ($\gtrsim 20$) dimensions often impractical
 - Incorporating gradients, several local BOs can help [Padidar, NeurIPS 2021]
 - **Neural network surrogates:**
 - Provides differentiable model
 - Likely only feasible within a limited configuration space (e.g., W7-X operating space)
 - **Optimization with data-driven subgrid or fluid closure models:**
 - If geometry independent, may not suffer from curse of dimensionality
 - e.g., improved gyrofluid closure for EP instabilities

Recent progress largely made through “physics-reduced” models

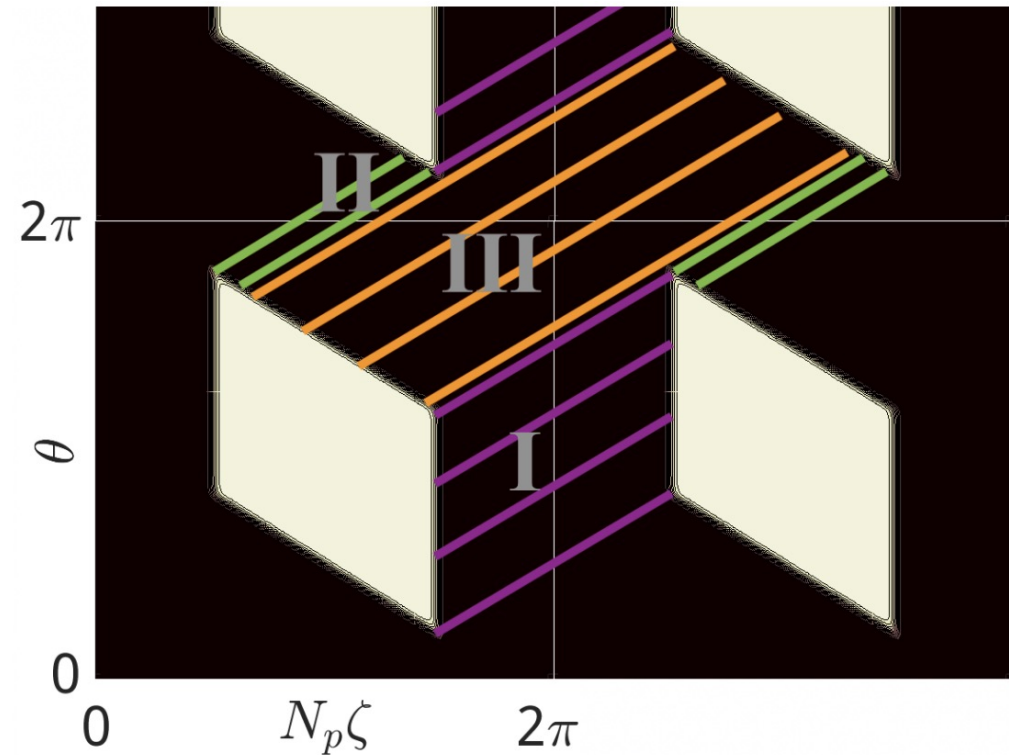
... but sometimes it pays off to attack the full problem

- Direct optimization of collisionless particle losses



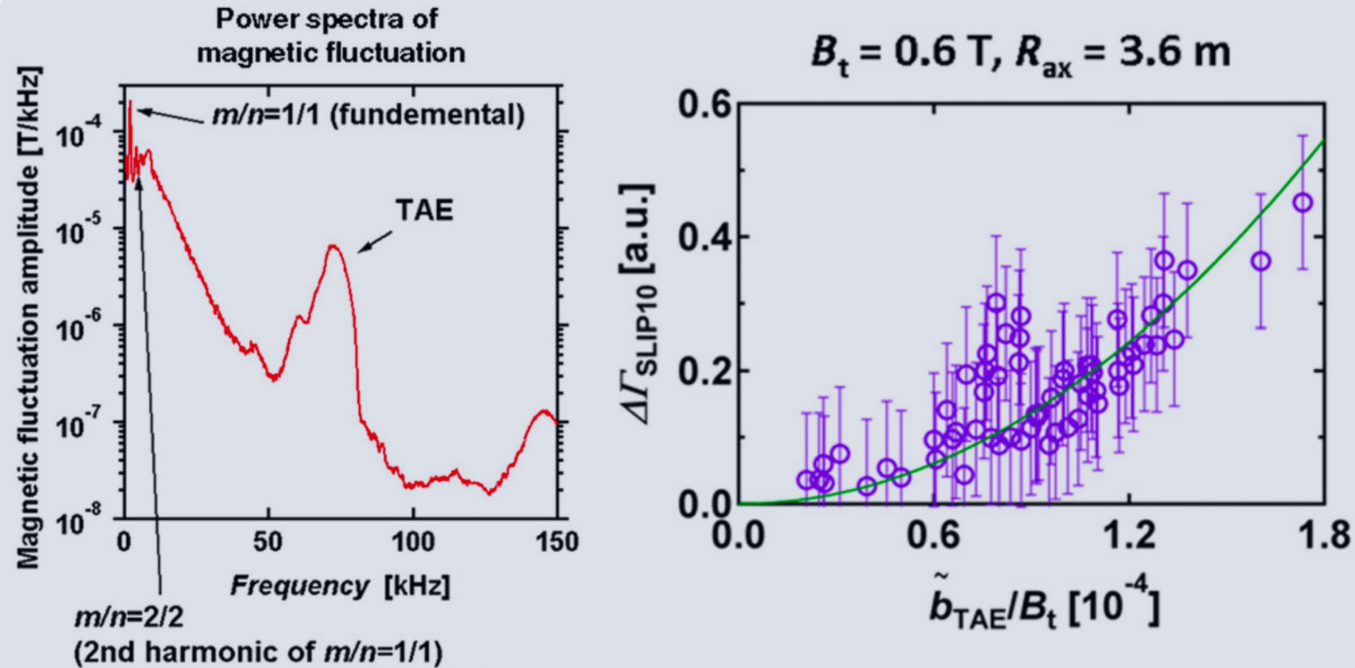
Bindel et al, *PPCF* 65 (2024).

- Discovery of new classes of optimized stellarators \rightarrow *piecewise omnigenity*



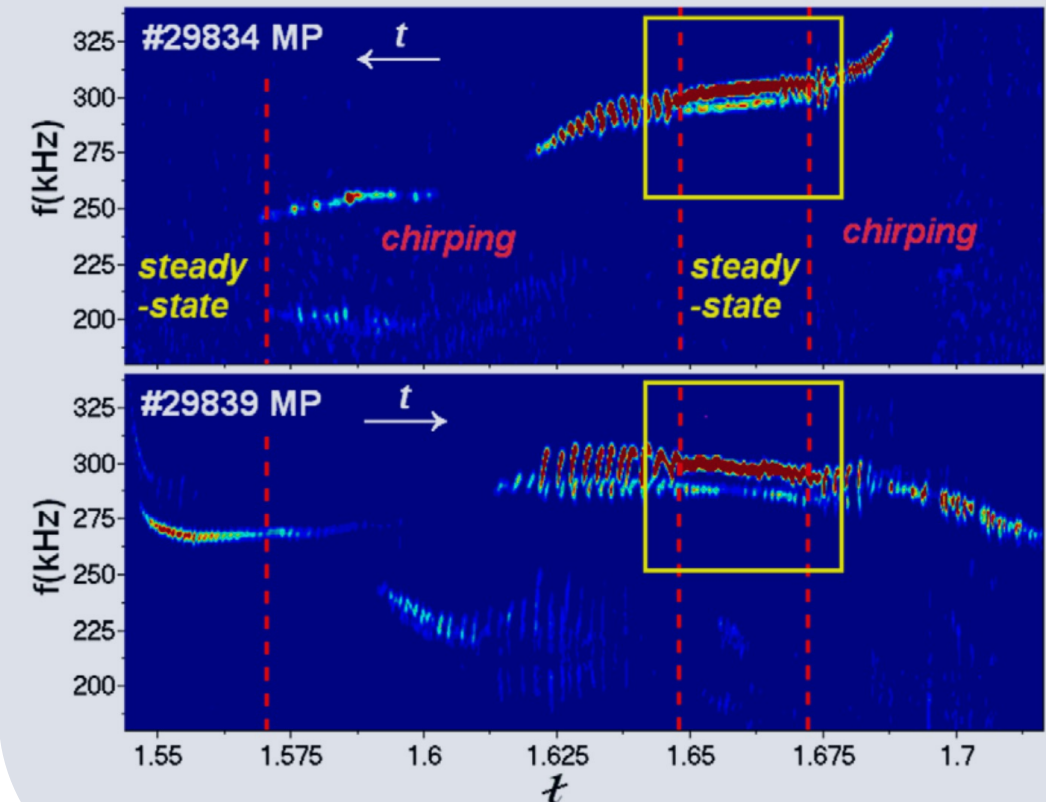
Velasco et al, *PRL* 133 (2024).

TAE-induced diffusive transport on LHD



Ogawa et al, *Nucl. Fusion* 50 (2010).

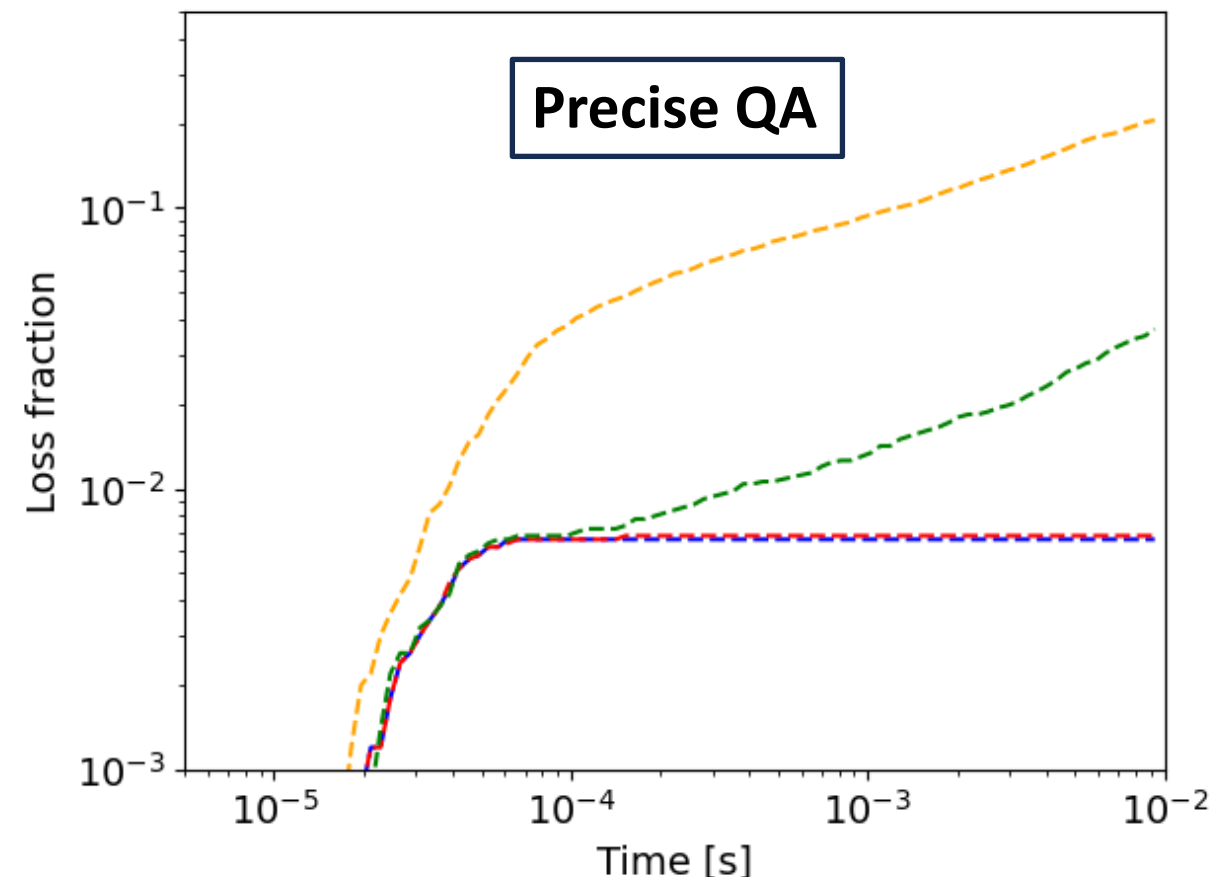
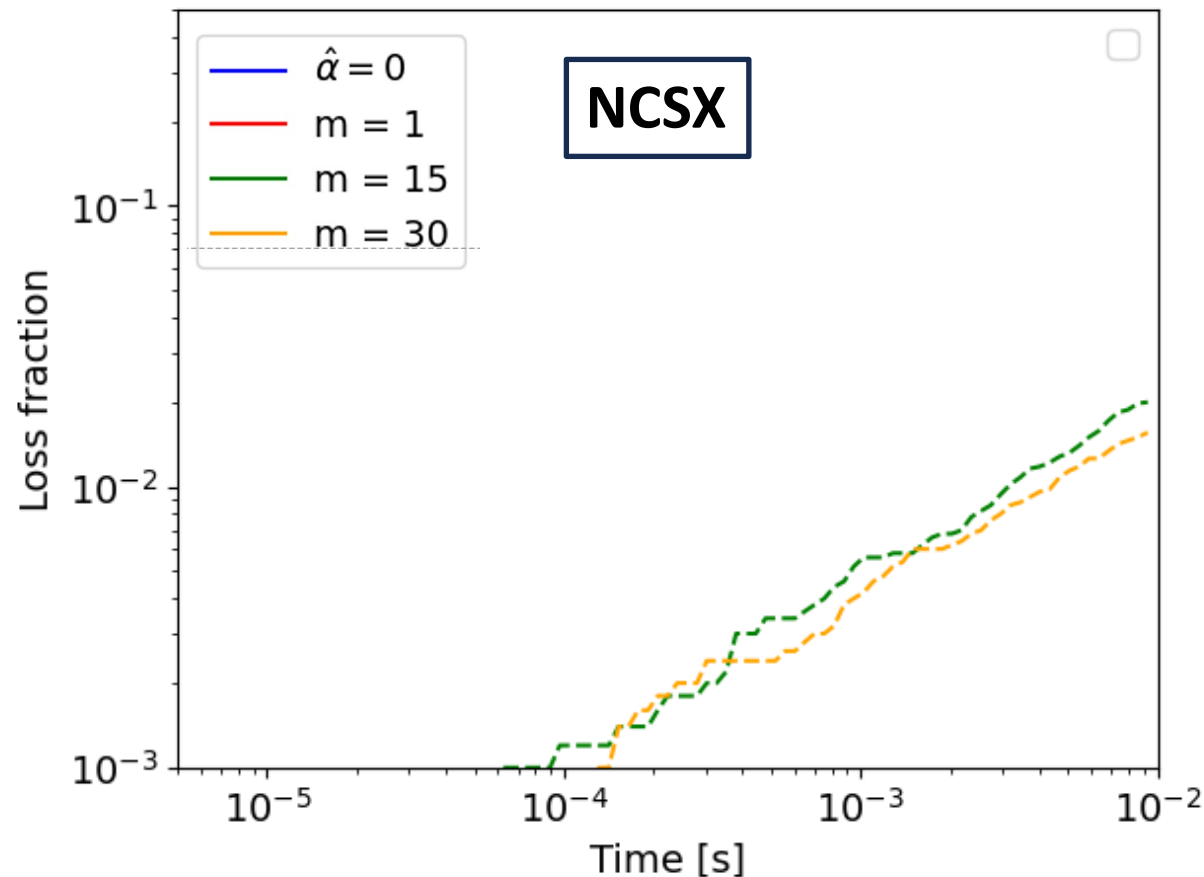
Transition between chirping and steady frequency on TJ-II



Melnikov et al, *Nucl. Fusion* 56 (2016).

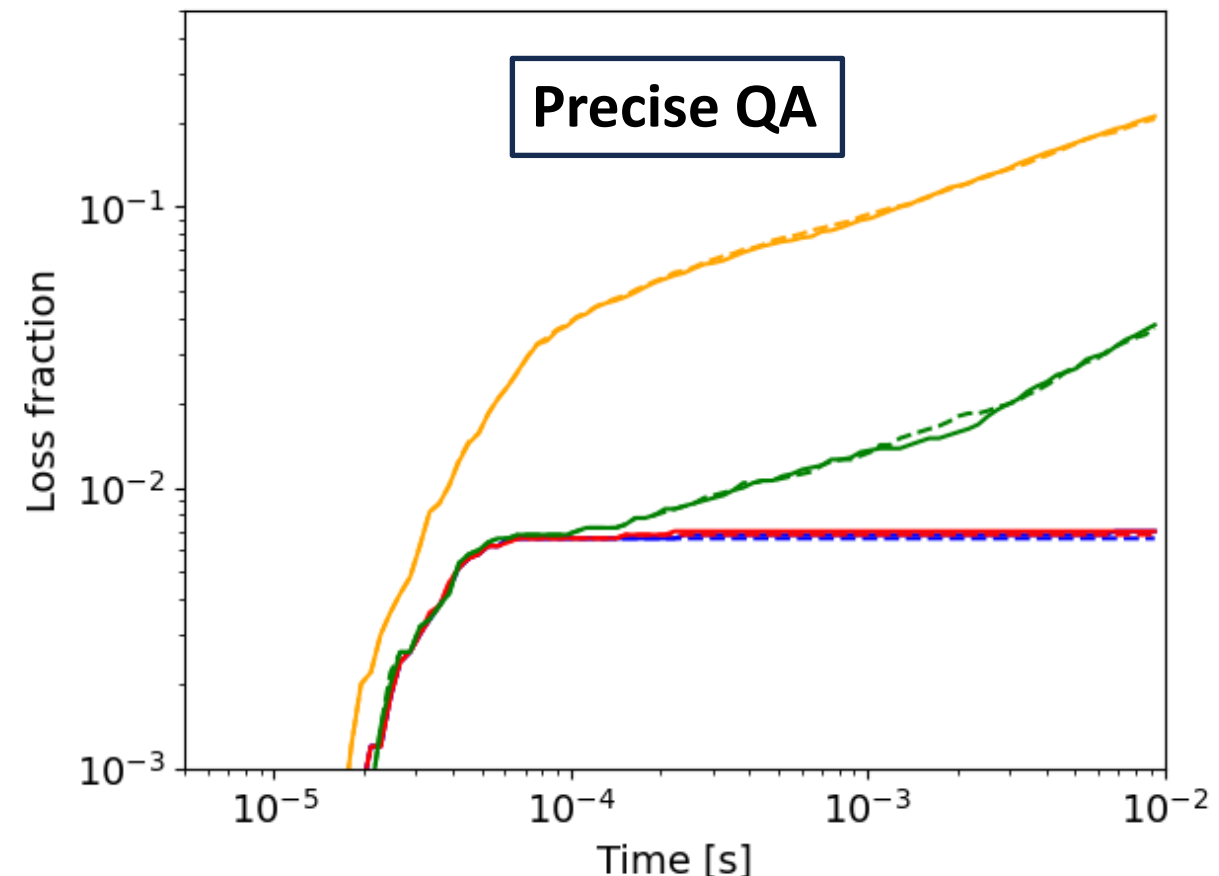
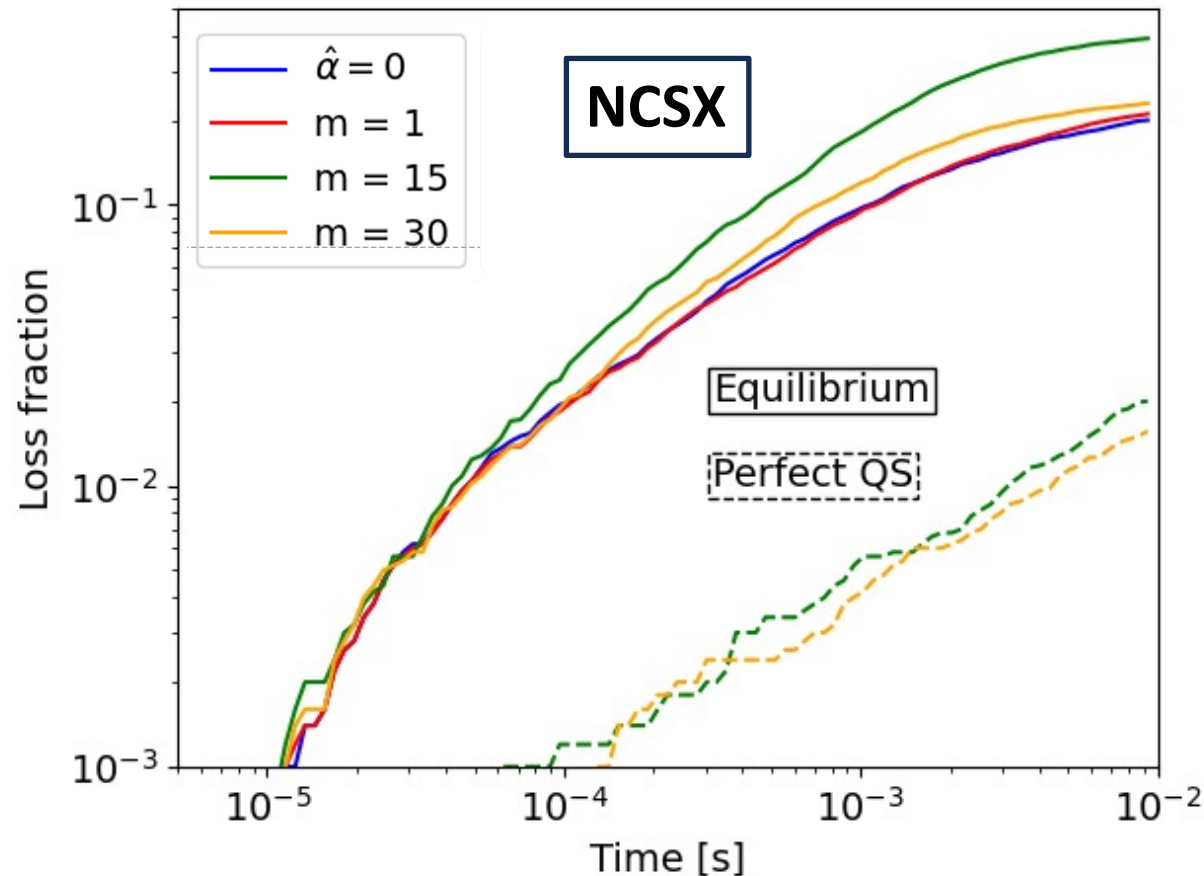
- Monte-Carlo analysis of collisionless 3.5 MeV alpha transport
- Resonant AE w/ $\delta \mathbf{B} \cdot \nabla \psi \sim 10^{-3}$ [Hsu & Sigmar, 1992]

Paul et al, *J. Plasma Phys.* 89 (2023).



- Monte-Carlo analysis of collisionless 3.5 MeV alpha transport
- Resonant AE w/ $\delta \mathbf{B} \cdot \nabla \psi \sim 10^{-3}$ [Hsu & Sigmar, 1992]
- Equilibrium destruction of drift surfaces causes enhanced losses

Paul et al, *J. Plasma Phys.* 89 (2023).



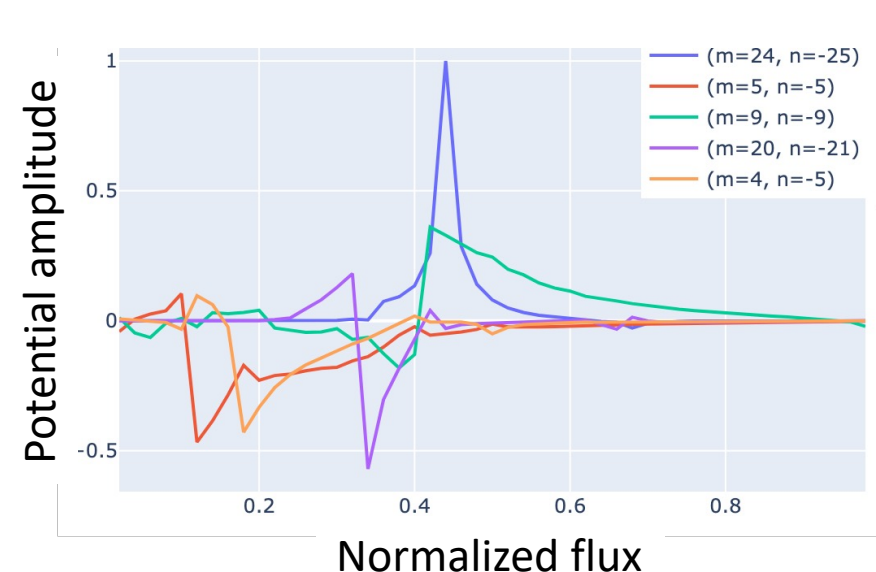
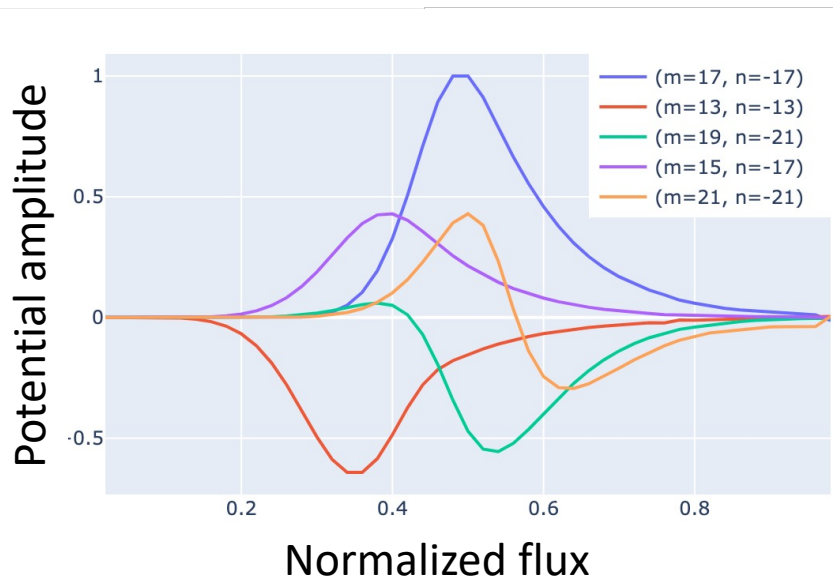
- The equations describing SAW can be derived from ideal MHD under the assumption of "reduced MHD" ($k_{\parallel}/k_{\perp} \ll 1$) and low beta [Salat & Tataronis, 2001]

$$B \nabla_{\parallel} \left(\frac{\nabla_{\perp}^2 (\nabla_{\parallel} \Phi)}{B} \right) + \frac{\omega^2 \nabla_{\perp}^2 \Phi}{v_A^2} = 0$$

- The equations describing SAW can be derived from ideal MHD under the assumption of "reduced MHD" ($k_{\parallel}/k_{\perp} \ll 1$) and low beta [Salat & Tataronis, 2001]

$$B \nabla_{\parallel} \left(\frac{\nabla_{\perp}^2 (\nabla_{\parallel} \Phi)}{B} \right) + \frac{\omega^2 \nabla_{\perp}^2 \Phi}{v_A^2} = 0$$

- Eigenvalue problem for potential, Φ , with solutions that are **global** (i.e., extending in radius) or **local** (like a delta-function)



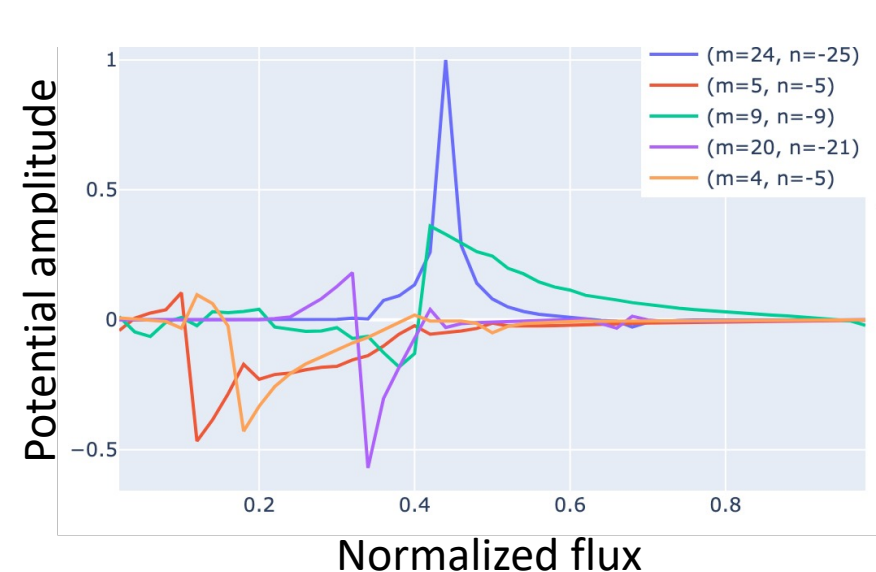
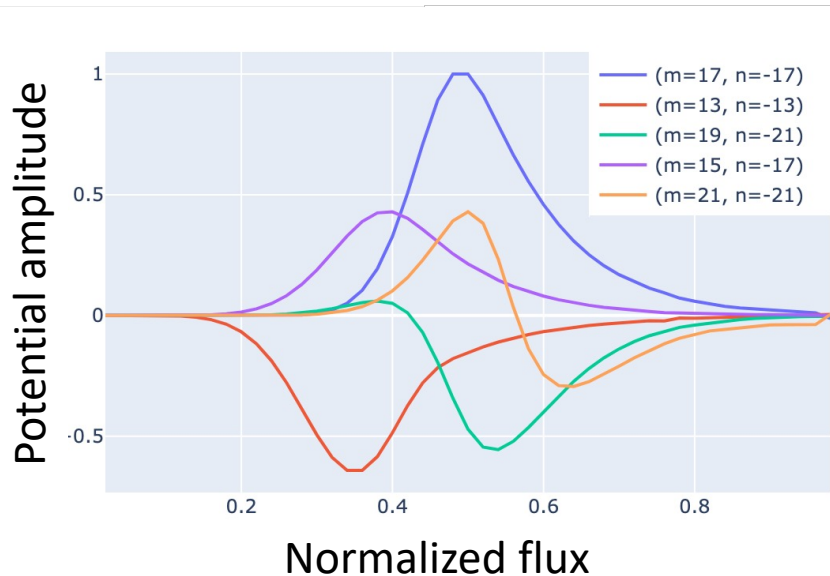
$$B \nabla_{\parallel} \left(\frac{\nabla_{\perp}^2 (\nabla_{\parallel} \Phi)}{B} \right) + \frac{\omega^2 \nabla_{\perp}^2 \Phi}{v_A^2} = 0$$



$$B \nabla_{\parallel} \left(\frac{|\nabla \psi|^2}{B} \nabla_{\parallel} \Phi \right) + \frac{\omega^2 |\nabla \psi|^2}{v_A^2} \Phi = 0$$

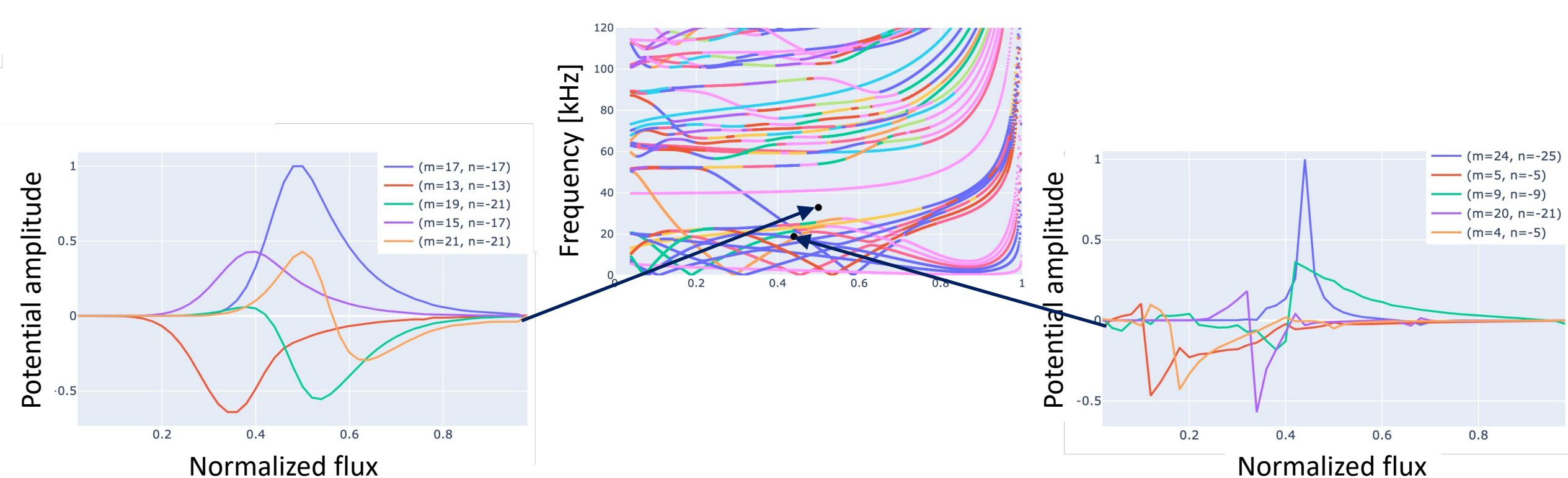
- Reduced MHD ($k_{\perp} \gg k_{\parallel}$) model for SAW
- Discrete modes **can be destabilized**

- Nullspace of second radial derivative
- Localized energy density → **heavily damped**

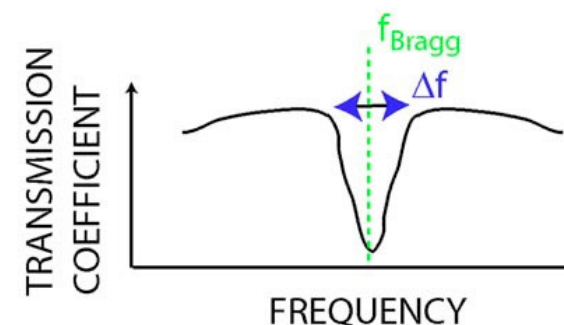
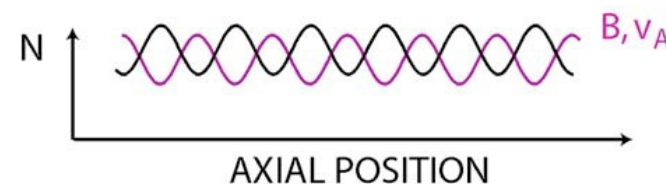
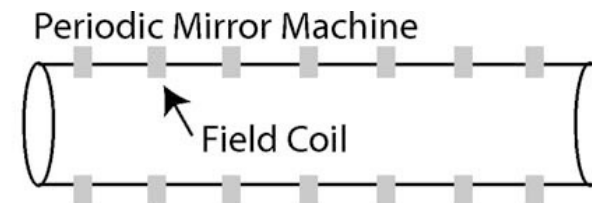
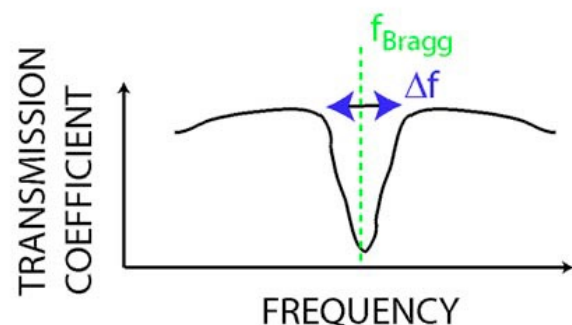
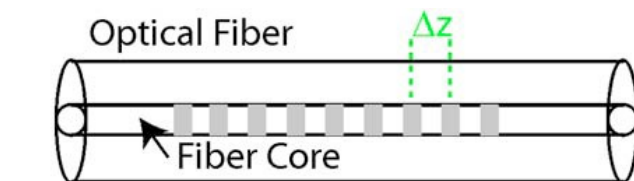


- We focus on localized continuum solutions, nullspace of highest-order radial derivative → **often the first step in assessing AE stability**

$$B \nabla_{\parallel} \left(\frac{|\nabla \psi|^2}{B} \nabla_{\parallel} \Phi \right) + \frac{\omega^2 |\nabla \psi|^2}{v_A^2} \Phi = 0$$



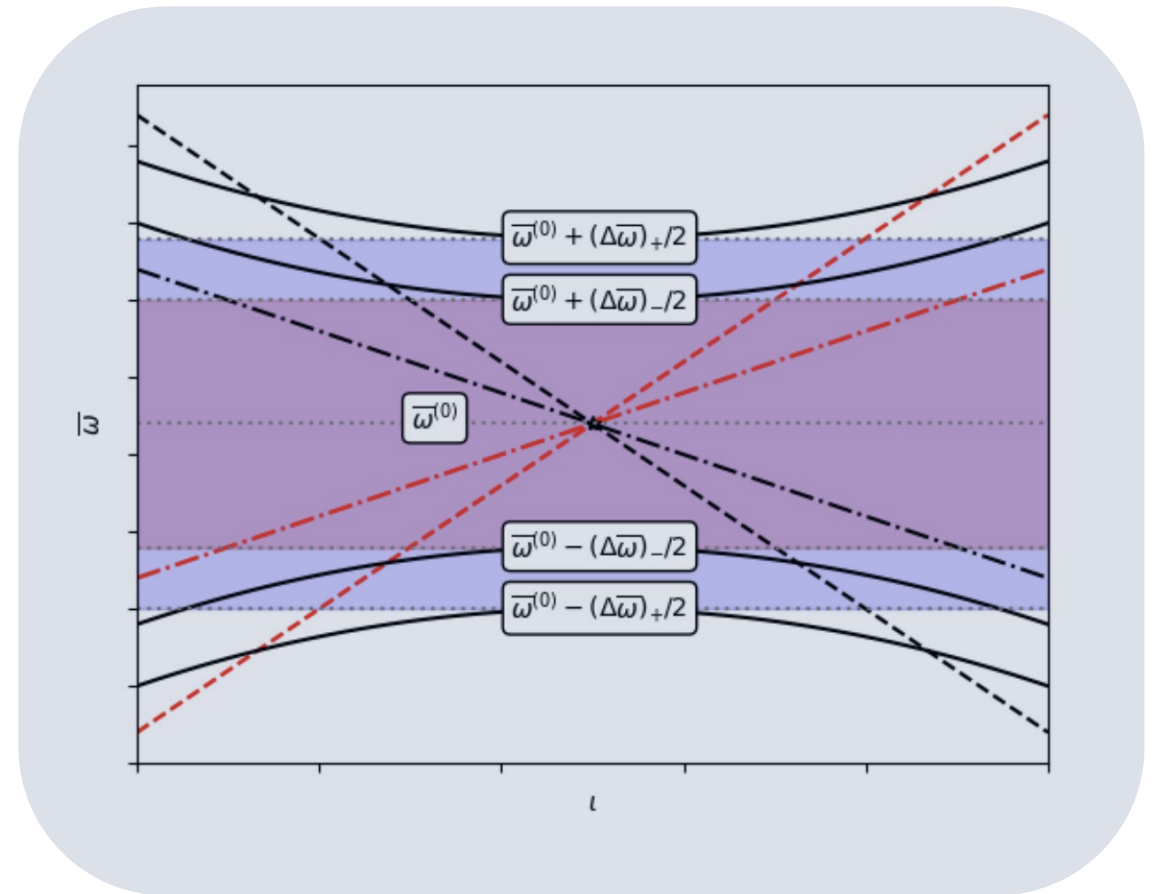
Heidbrink, *Phys. Plasmas* 15 (2008).



- Periodic modulation of index of refraction introduces **frequency gap**
 - Optical fiber \rightarrow transmission gap
 - Semiconductors \rightarrow band gap
- “Band gap engineering” by modifying material properties

Outline

- *Stellarator optimization and AI/ML*
- ***Perturbation theory for shear Alfvén continuum***
- *Can we manipulate the shear Alfvén continuum to avoid resonance?*



- Continuum equation in Boozer coordinates near magnetic axis:

$$\frac{1}{1 + \epsilon} \left(\frac{\partial}{\partial \zeta} + \iota_0 \frac{\partial}{\partial \theta} \right) \left[(1 + \epsilon) \left(\frac{\partial}{\partial \zeta} + \iota_0 \frac{\partial}{\partial \theta} \right) \Phi \right] + \bar{\omega}^2 \Phi = 0$$

- Expand in smallness of coupling parameter, $\epsilon = \frac{|\nabla\psi|^2}{\langle |\nabla\psi|^2 \rangle} - 1$

- Continuum equation in Boozer coordinates near magnetic axis:

$$\frac{1}{1 + \epsilon} \left(\frac{\partial}{\partial \zeta} + \iota_0 \frac{\partial}{\partial \theta} \right) \left[(1 + \epsilon) \left(\frac{\partial}{\partial \zeta} + \iota_0 \frac{\partial}{\partial \theta} \right) \Phi \right] + \bar{\omega}^2 \Phi = 0$$

- Expand in smallness of coupling parameter, $\epsilon = \frac{|\nabla\psi|^2}{\langle |\nabla\psi|^2 \rangle} - 1$
- **Degenerate perturbation theory** is required (analogous to, e.g. Stark effect)
- Goal:
 - *Analytic expressions for the gap widths*
 - *Understand interaction between gaps in 3D geometry*

Lowest order: No coupling (i.e., cylinder)

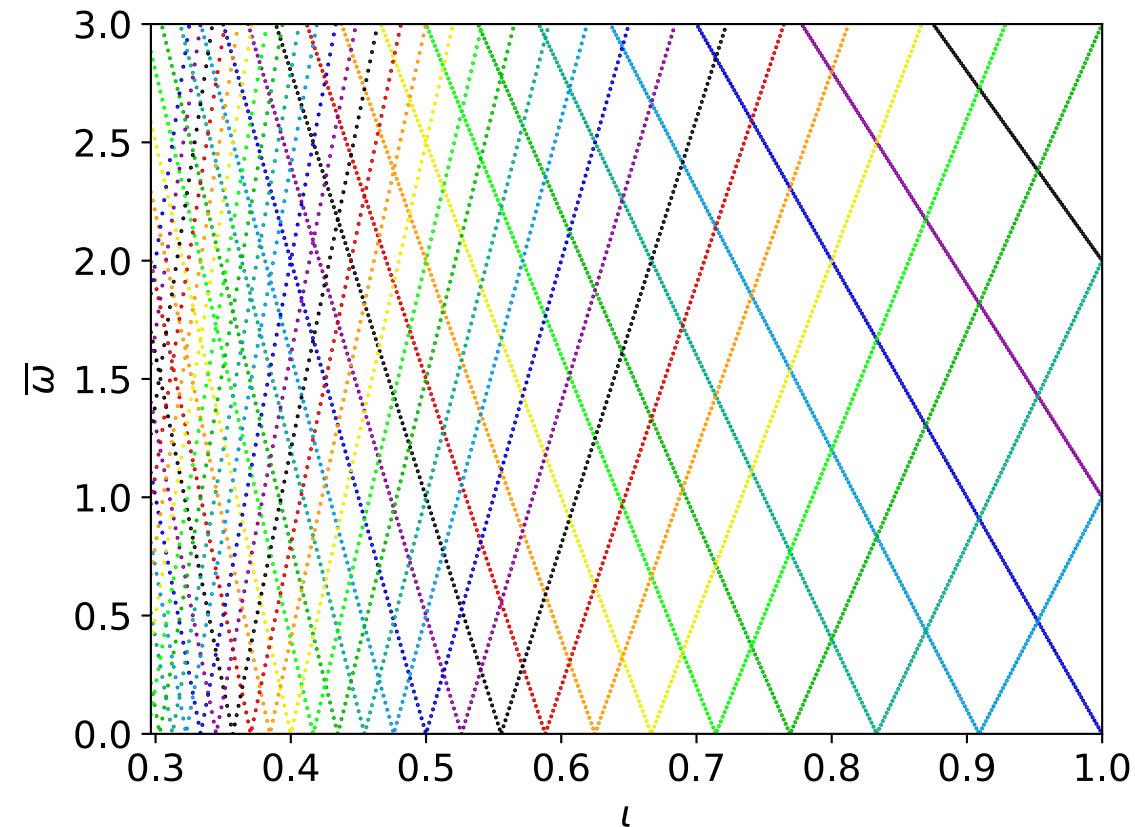
$$\left(\frac{\partial}{\partial \zeta} + \iota_0 \frac{\partial}{\partial \theta}\right) \left[\left(\frac{\partial}{\partial \zeta} + \iota_0 \frac{\partial}{\partial \theta}\right) \Phi_j^{(0)} \right] + \left(\bar{\omega}_j^{(0)}\right)^2 \Phi_j^{(0)} = 0$$

- Eigenfunctions:

$$\Phi_j^{(0)} = \Phi_{m_j, n_j} e^{i(m_j \theta - n_j \zeta + \omega t)}$$

- Normalized frequencies:

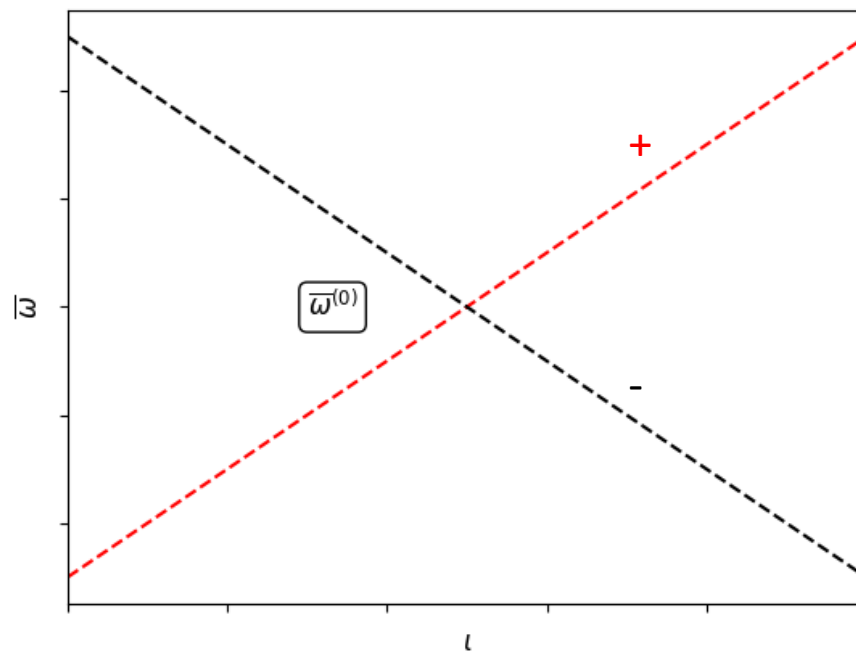
$$\left(\bar{\omega}_j^{(0)}\right)^2 = (\iota_0 m_j - n_j)^2$$



$$\left(\frac{\partial}{\partial \zeta} + \iota_0 \frac{\partial}{\partial \theta}\right)^2 \Phi^{(1)+} \left[\left(\frac{\partial}{\partial \zeta} + \iota_0 \frac{\partial}{\partial \theta}\right) \epsilon\right] \left[\left(\frac{\partial}{\partial \zeta} + \iota_0 \frac{\partial}{\partial \theta}\right) \Phi^{(0)}\right] + \left(\bar{\omega}^{(0)}\right)^2 \Phi^{(1)} + \left(\bar{\omega}^{(1)}\right) \Phi^{(0)} = 0$$

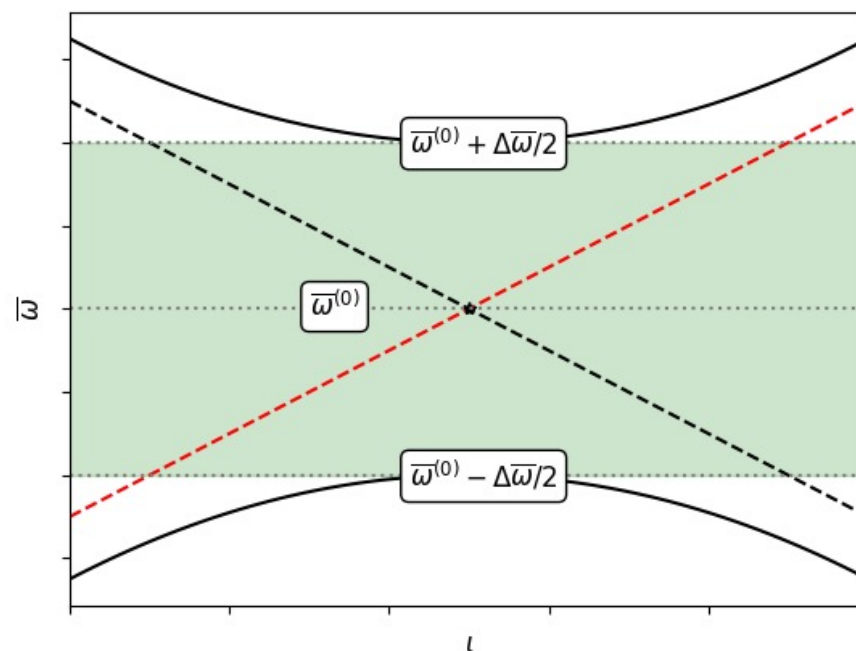
- Degeneracy implies “crossing” of unperturbed frequencies: $\Phi^{(0)} = \alpha_j \Phi_j^{(0)} + \alpha_k \Phi_k^{(0)}$

$$\left(\bar{\omega}_j^{(0)}\right)^2 = \left(\bar{\omega}_k^{(0)}\right)^2 \rightarrow \iota_0 m_j - n_j = \pm(\iota_0 m_k - n_k)$$



- For “co-propagating” degeneracy (+ root) $\rightarrow \iota_0 = \Delta n / \Delta m$ (**only in 3D**)

$$\bar{\omega}^{(1)} = 0$$



Gap width:

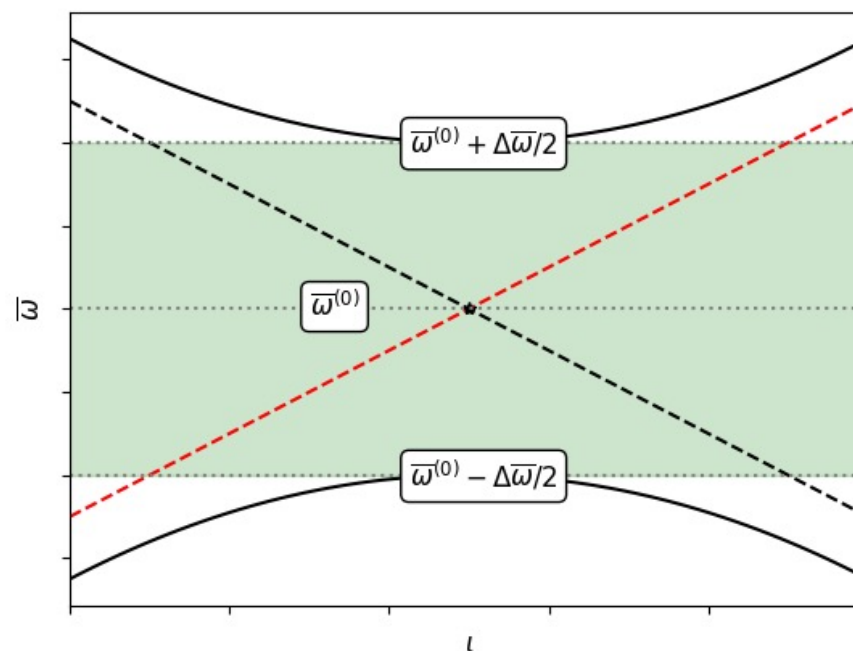
$$\Delta\omega = 2|\epsilon_{\Delta m, \Delta n}| \bar{\omega}^{(0)}$$

- For "co-propagating" degeneracy (+ root) $\rightarrow \iota_0 = \Delta n / \Delta m$ (**only in 3D**)

$$\bar{\omega}^{(1)} = 0$$

- For "counter-propagating" degeneracy (- root) \rightarrow **frequency splitting**

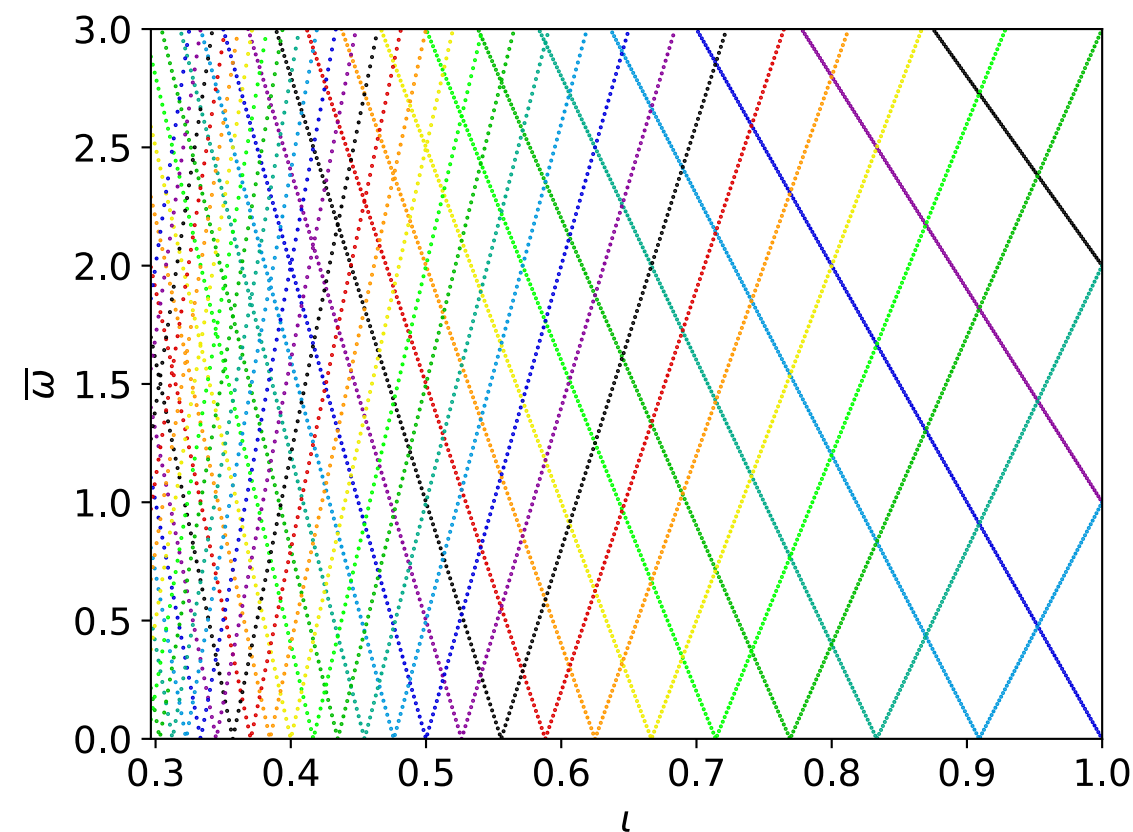
$$\bar{\omega}^{(1)} = 2|\epsilon_{\Delta m, \Delta n}| \bar{\omega}^{(0)}$$



Gap width:

$$\Delta\omega = 2|\epsilon_{\Delta m, \Delta n}| \bar{\omega}^{(0)}$$

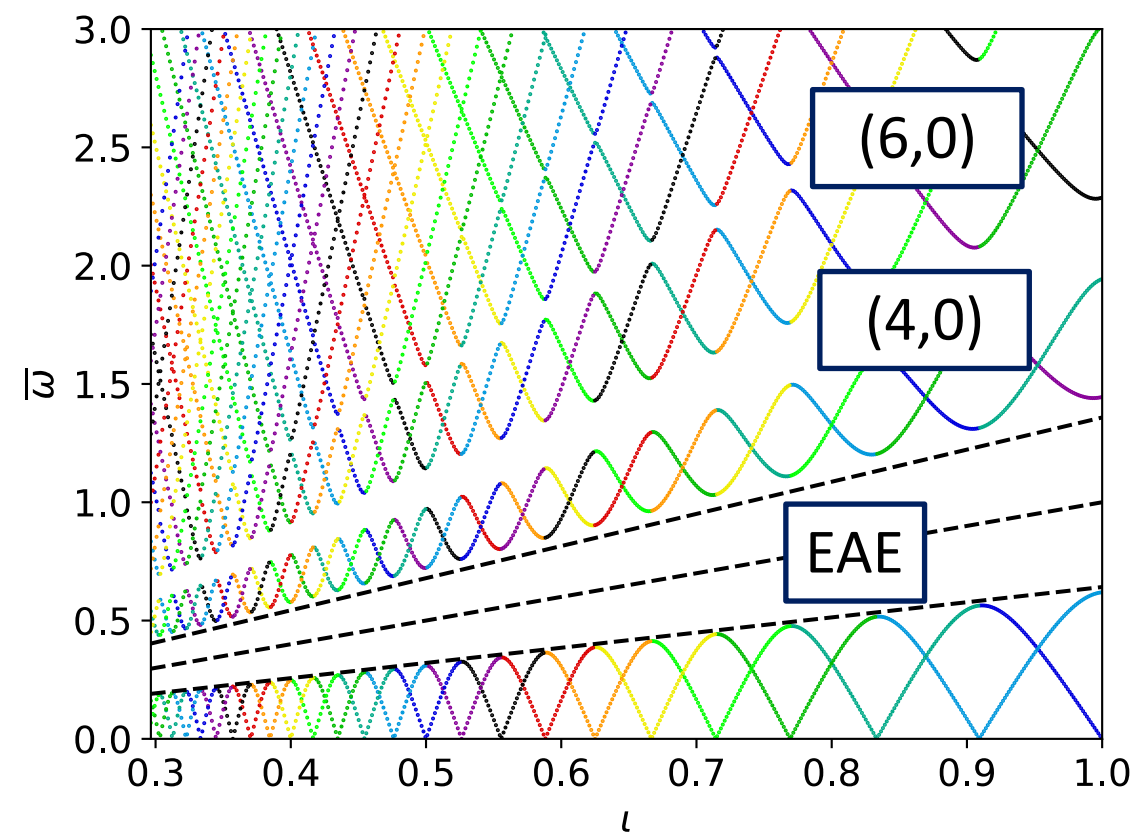
- Classify gaps by coupling mode numbers $(\Delta m, \Delta n)$
- In axisymmetry:
 - TAE ($\Delta m = 1, \Delta n = 0$)
 - EAE ($\Delta m = 2, \Delta n = 0$)
 - (... higher-order poloidal shaping)
- In stellarators, also:
 - HAE ($\Delta m \neq 0, \Delta n \neq 0$)
 - MAE ($\Delta m = 0, \Delta n \neq 0$)



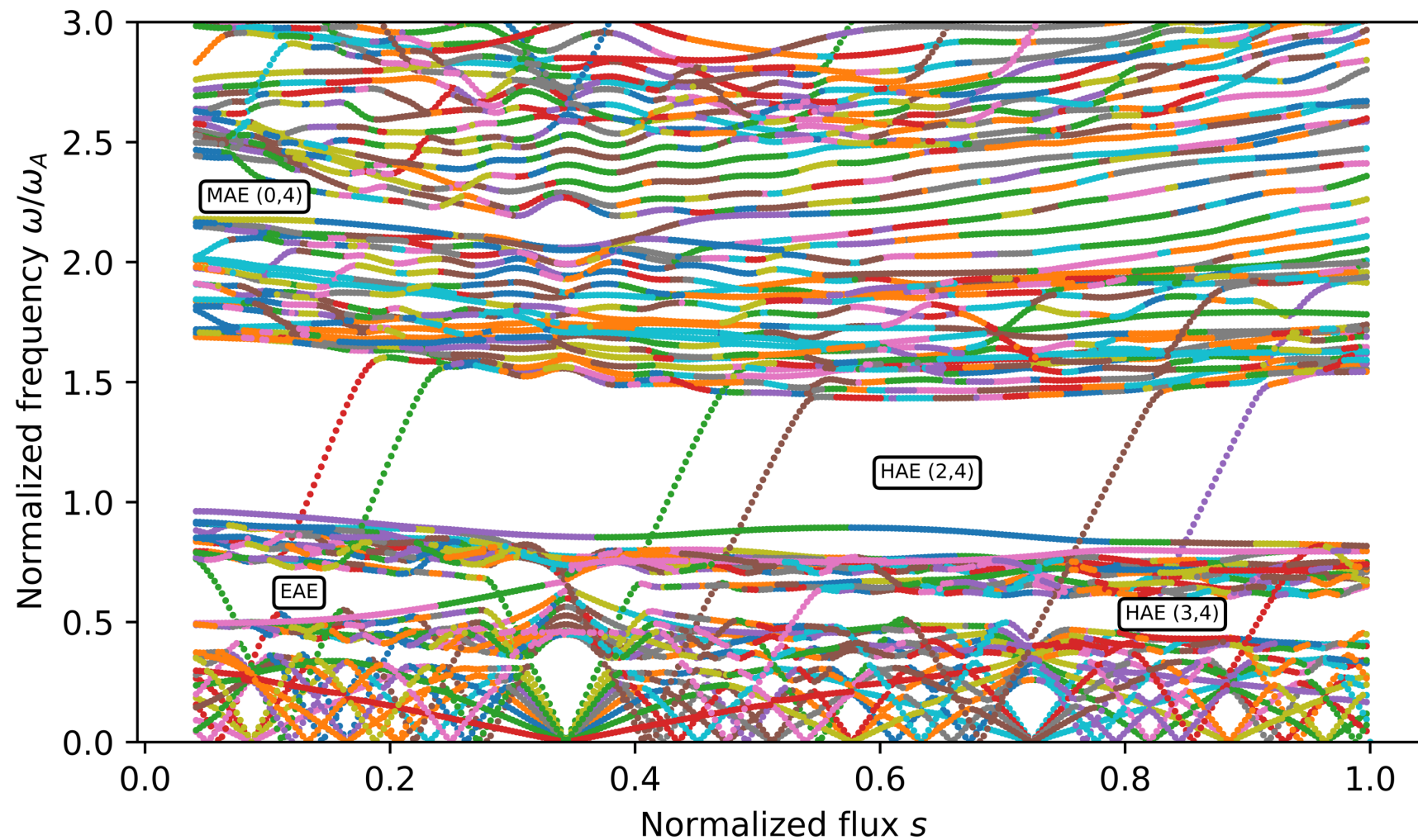
- Classify gaps by coupling mode numbers $(\Delta m, \Delta n)$
- In axisymmetry:
 - TAE ($\Delta m = 1, \Delta n = 0$)
 - EAE ($\Delta m = 2, \Delta n = 0$)
 - (... higher-order poloidal shaping)
- In stellarators, also:
 - HAE ($\Delta m \neq 0, \Delta n \neq 0$)
 - MAE ($\Delta m = 0, \Delta n \neq 0$)

Gaps remain separated in 2D:

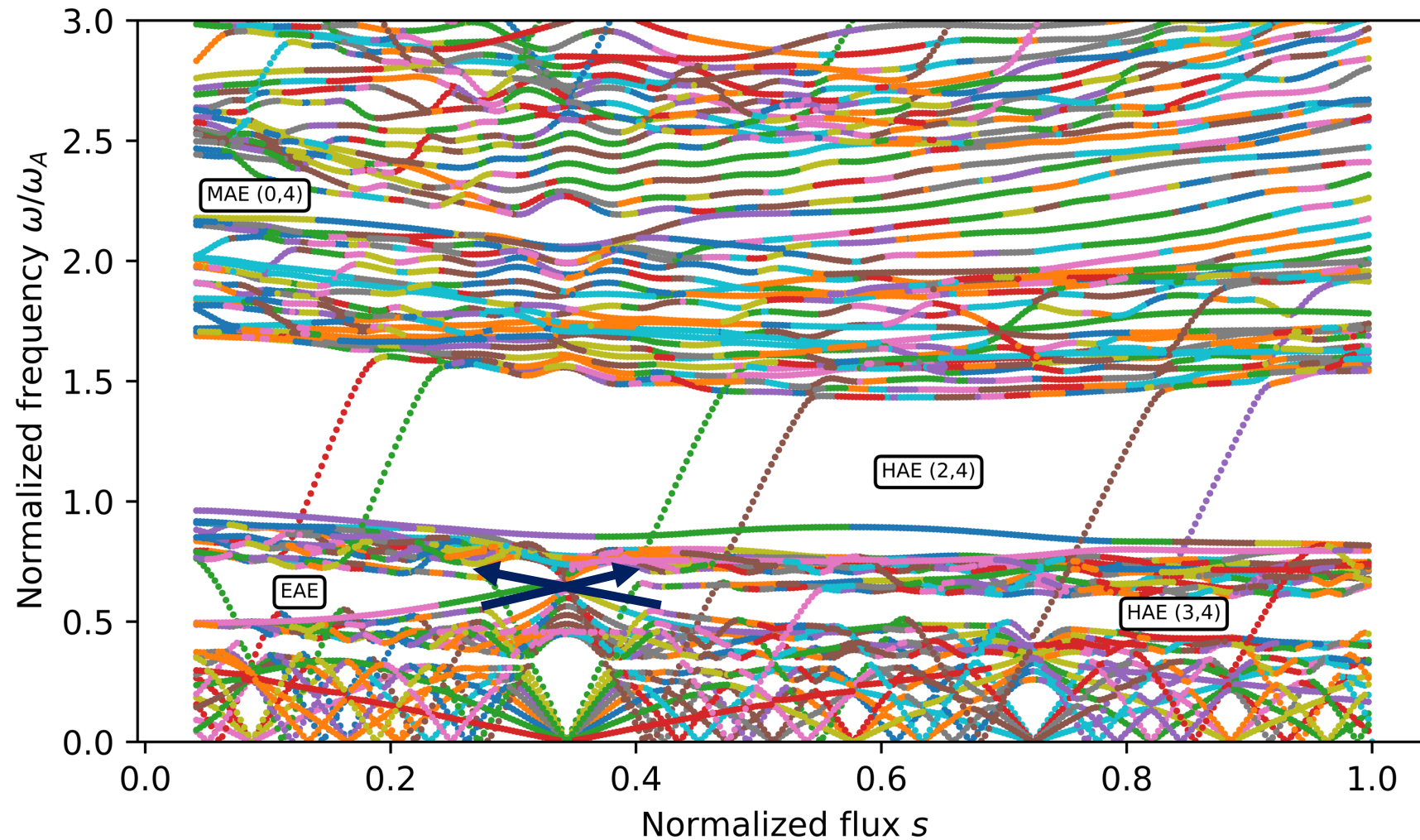
$$\overline{\omega}^{(0)} = |\iota_0 \Delta m - \Delta n|/2$$



Stellgap [Spong, 2003] calculations by A. Hyder

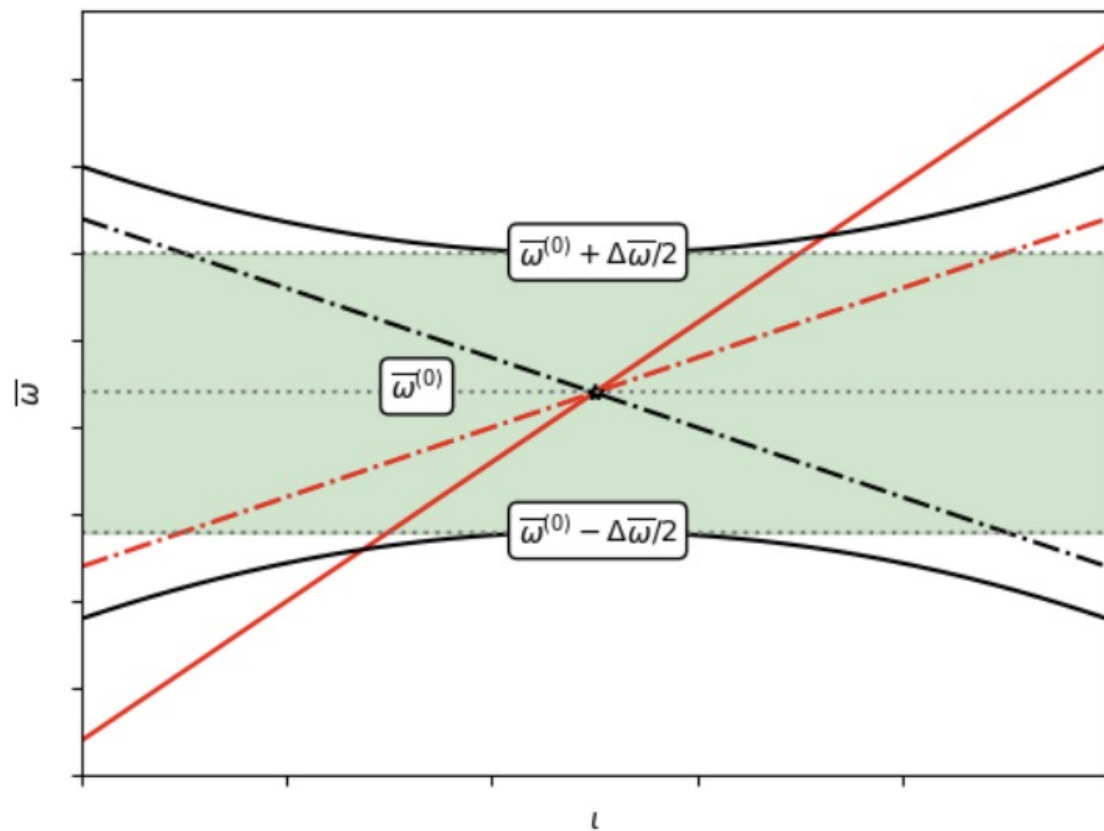


Stellgap [Spong, 2003] calculations by A. Hyder

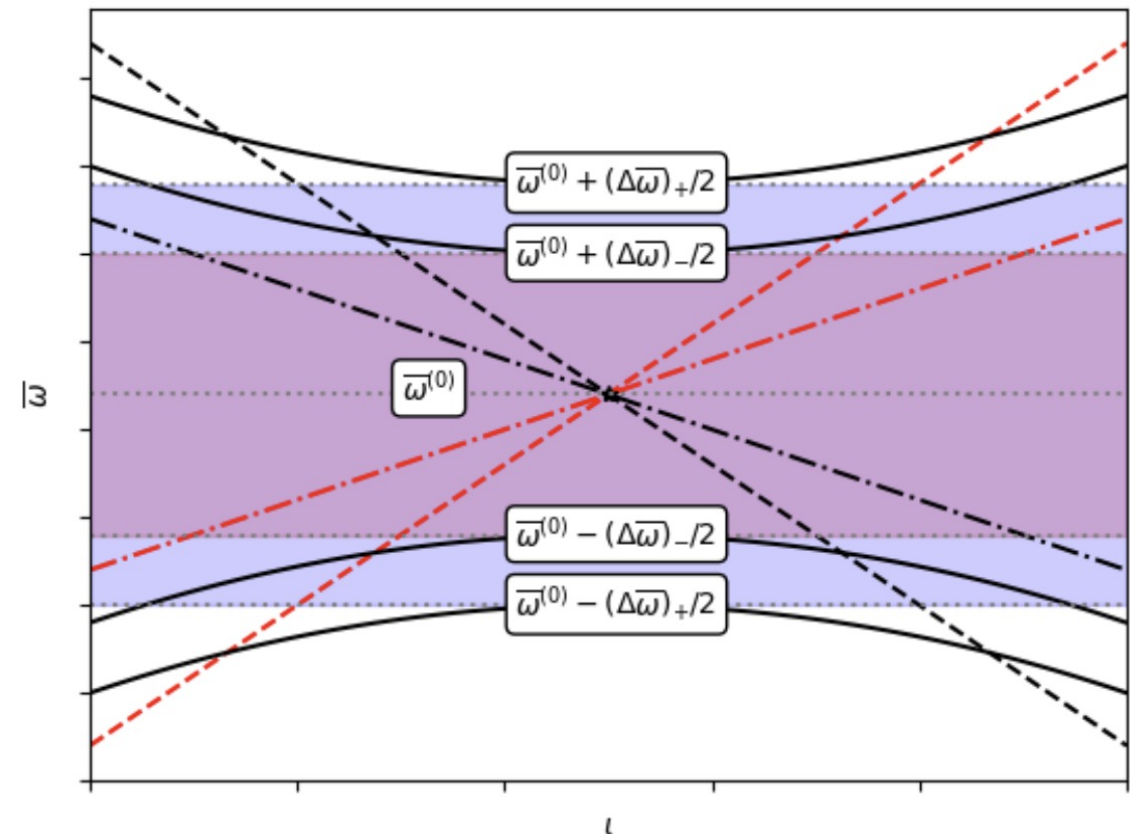


Higher-order crossings possible in 3D systems

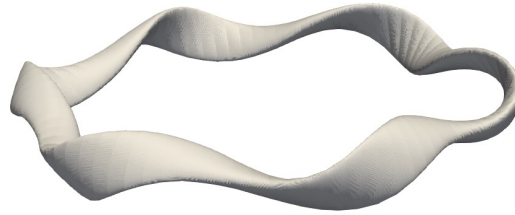
Two co-propagating, third counter-propagating: one “**gap crossing**” mode



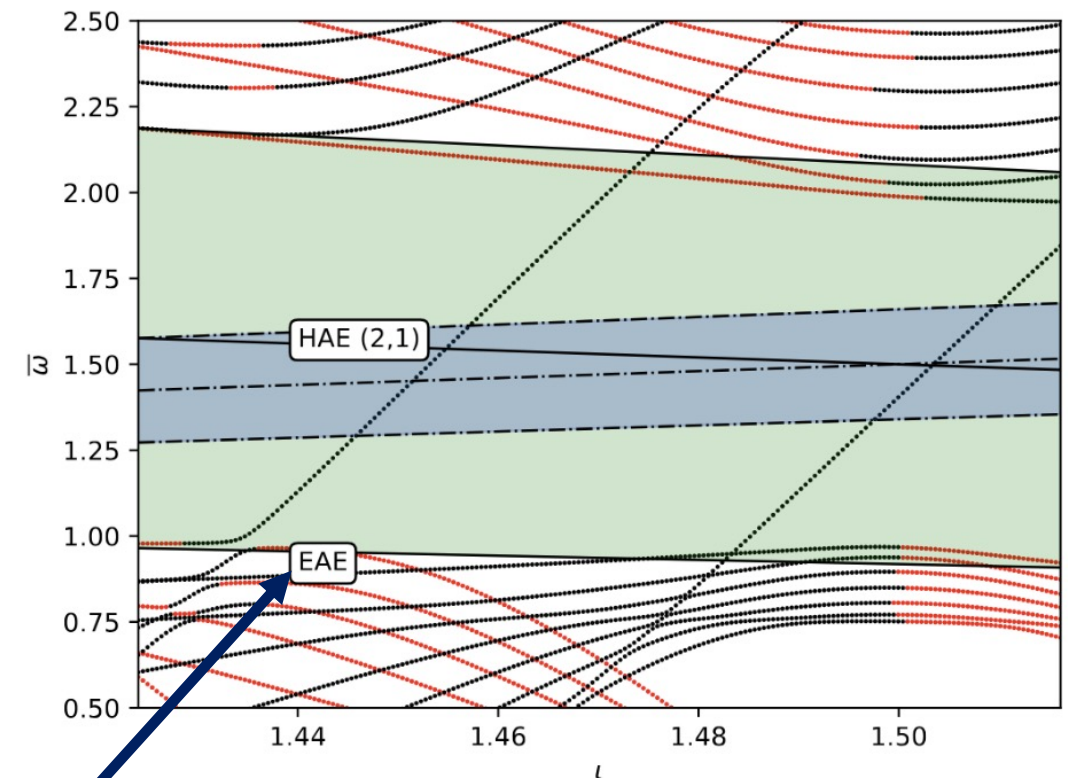
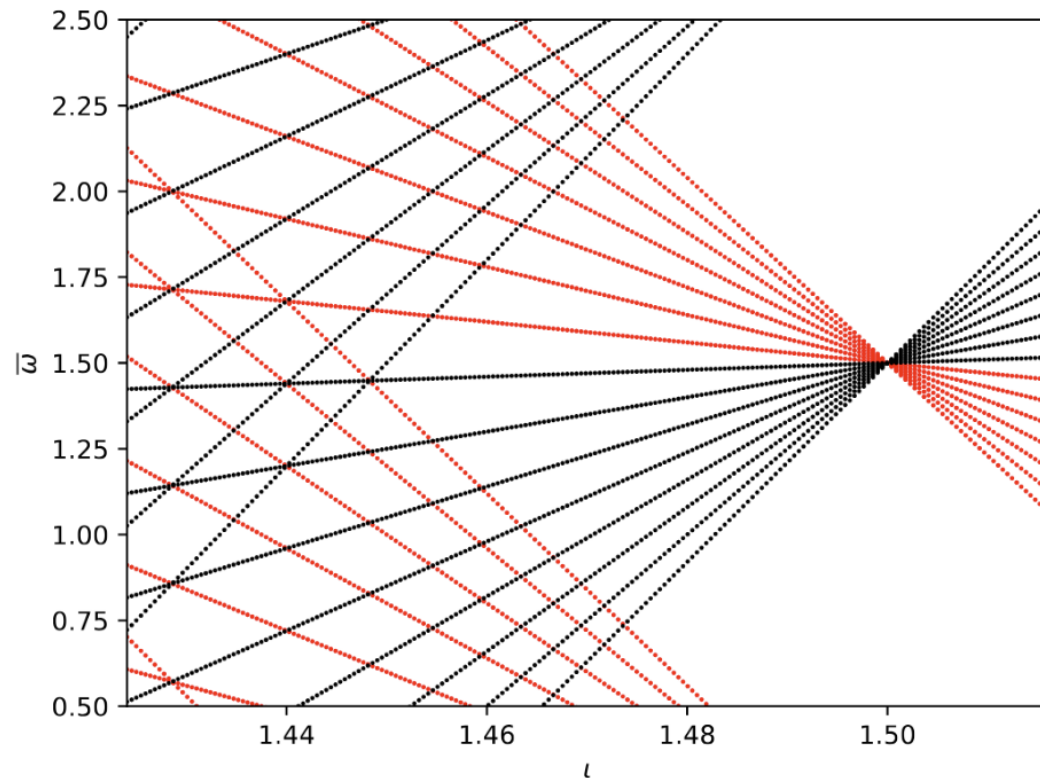
Two counter-propagating pairs: frequency of each shift in “**nested gaps**”



Nührenberg-Zille configuration: 15-way crossing



J. Nührenberg and R. Zille, *Phys. Lett. A* (1988)



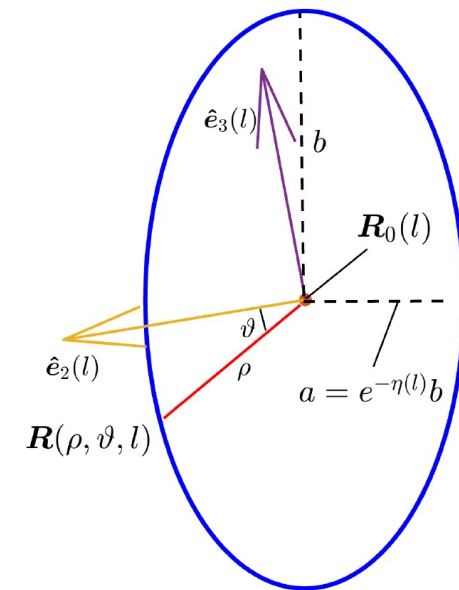
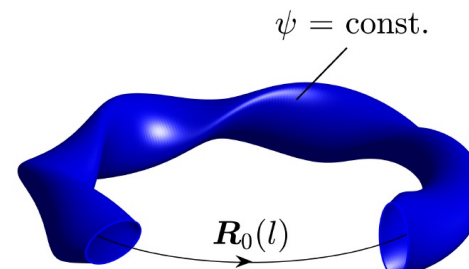
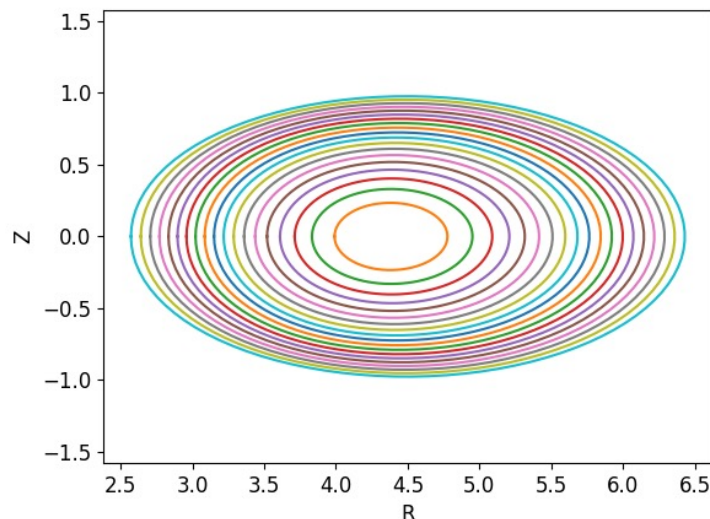
"Gap repulsion" [Y. I. Kolesnichenko, 2001]

- Near-axis model for the flux-surface compression factor, $|\nabla\psi|^2$

$$|\nabla\psi|^2 = r^2\Psi_2 + r^3\Psi_3 + \mathcal{O}(r^4)$$

- Defining coordinate system oriented with ellipse axes, $x = a \cos \vartheta, y = b \sin \vartheta$

$$\Psi_2 = B_0^2 \frac{p - \sqrt{p^2 - 4} \cos 2\vartheta}{2}$$



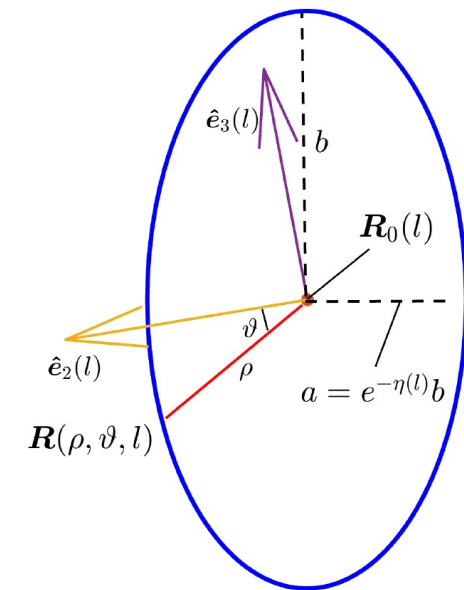
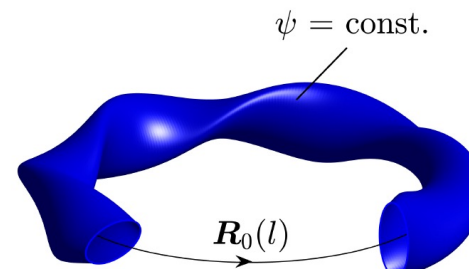
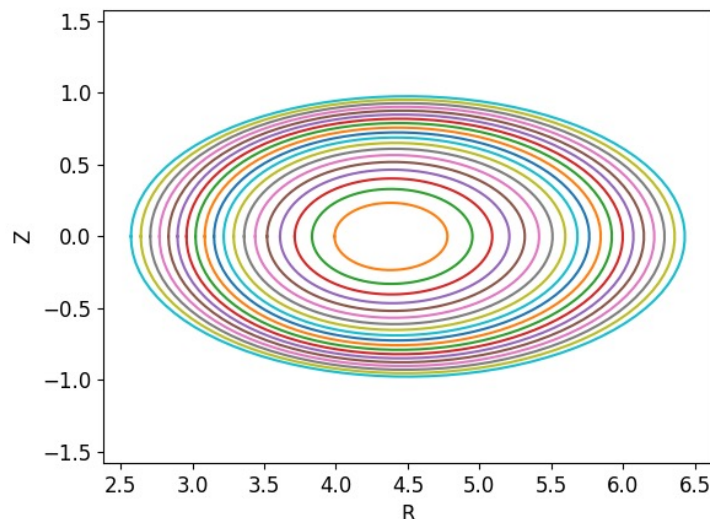
- Near-axis model for the flux-surface compression factor, $|\nabla\psi|^2$

$$|\nabla\psi|^2 = r^2\Psi_2 + r^3\Psi_3 + \mathcal{O}(r^4)$$

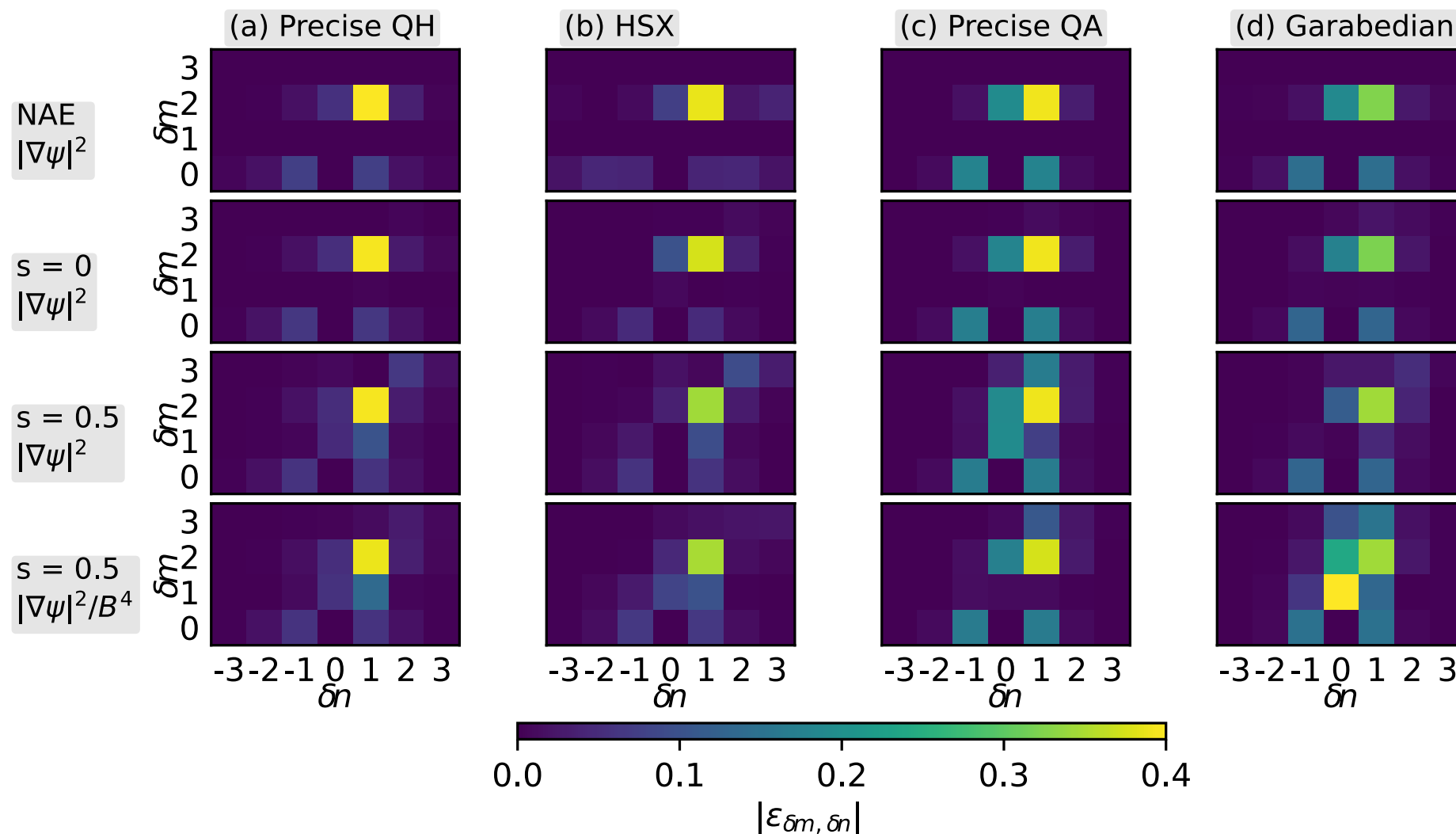
- Defining coordinate system oriented with ellipse axes, $x = a \cos \vartheta, y = b \sin \vartheta$

$$\Psi_2 = B_0^2 \frac{p - \sqrt{p^2 - 4} \cos 2\vartheta}{2}$$

- Given that ellipse typically makes one half-rotation per field period, **produces helical ($m = 2, n = N_P$) coupling** [Kolesnichenko, 2001]

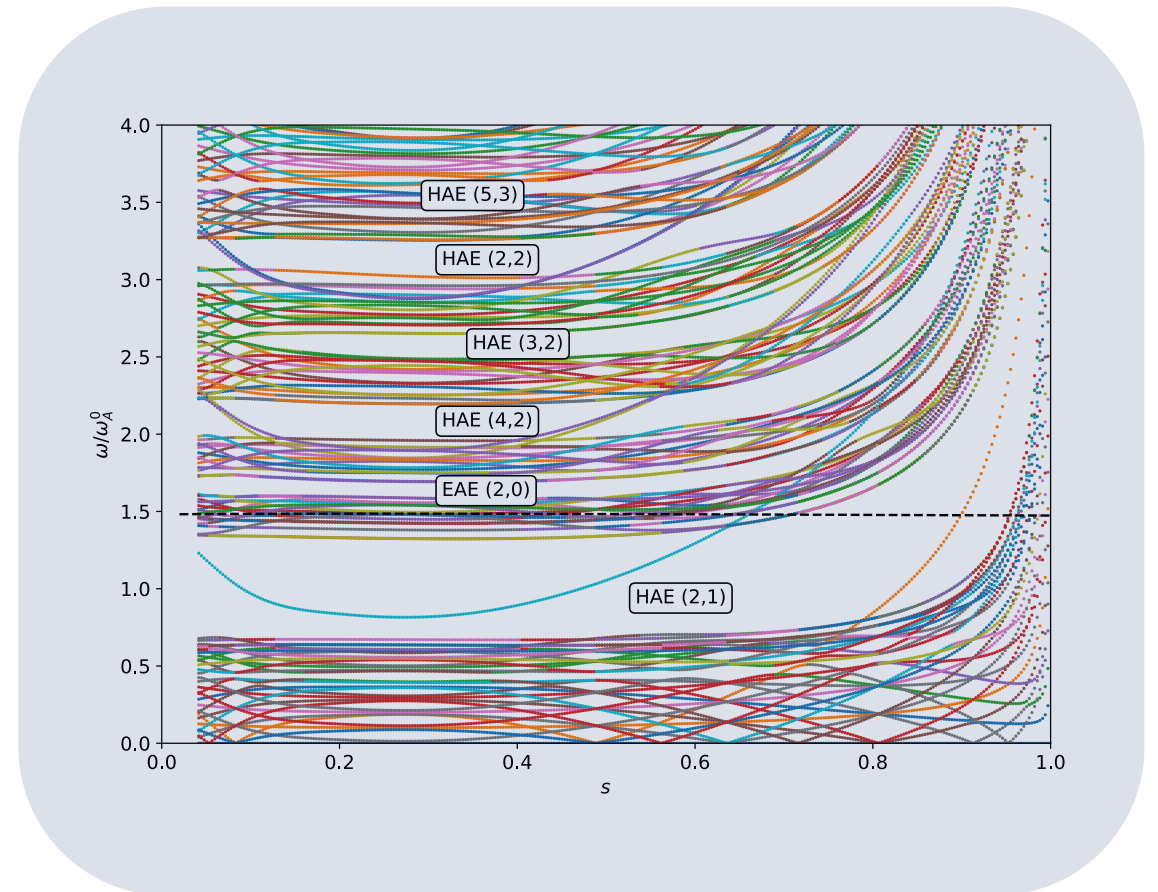


- Toroidal variation of elongation and curvature drive MAE and EAE modes



Outline

- *Stellarator optimization and AI/ML*
- *Perturbation theory for shear Alfvén continuum*
- ***Can we manipulate the shear Alfvén continuum to avoid resonance?***



- Assume configuration close to QS with $B(\psi, \chi = \theta - N\zeta)$
- Passing particle dynamics characterized by transit frequency profiles $\omega_\theta, \omega_\zeta, \omega_\chi$

e.g., $\omega_\theta = \langle \dot{\theta} \rangle$

- Assume configuration close to QS with $B(\psi, \chi = \theta - N\zeta)$
- Passing particle dynamics characterized by transit frequency profiles $\omega_\theta, \omega_\zeta, \omega_\chi$

$$\text{e.g., } \omega_\theta = \langle \dot{\theta} \rangle$$

- Resonance condition with SAW s.t. wave phase is constant in particle frame:

$$\Omega_l = (m + l)\omega_\chi - (n - Nm)\omega_\zeta + \omega = 0$$

- Coupling through magnetic drifts introduces multiple resonant surfaces through l
- Strongest resonance for $l = 0, 1$

- At typical reactor scale (e.g., HSR418), $n_i \approx 3 \times 10^{20}$ m/s, $B \approx 5$ T \rightarrow
 $\omega_A/\omega_\zeta \approx 1/4$ at 3.5 MeV
 \rightarrow Strong passing resonance requires $\omega/\omega_A > 1$

- At typical reactor scale (e.g., HSR418), $n_i \approx 3 \times 10^{20}$ m/s, $B \approx 5$ T \rightarrow $\omega_A/\omega_\zeta \approx 1/4$ at 3.5 MeV
 \rightarrow Strong passing resonance requires $\omega/\omega_A > 1$

$$\bar{\omega} > |\iota - N|/2$$

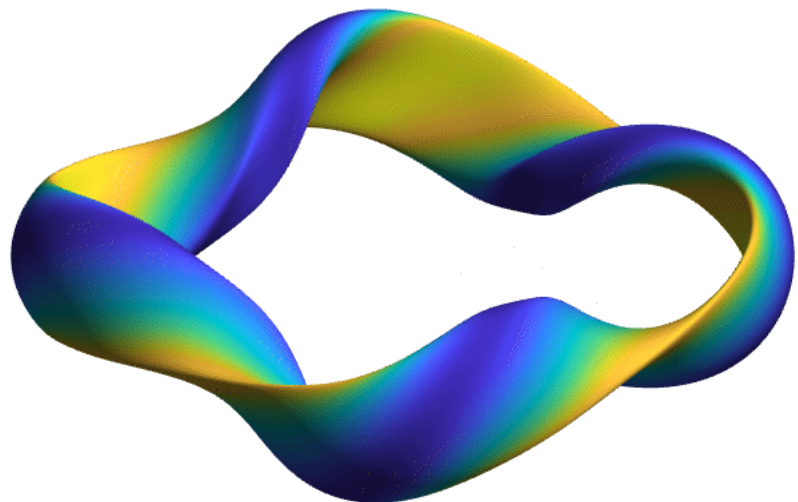
- **Strategy:**
 - Preferentially promote low-frequency gaps to
 - ✓ Avoid resonance at birth energy
 - ✓ Avoid wide gaps ($\Delta\omega \propto \omega$)
 - Reduce ω_A (e.g., high-density, low field)

- Fixed-boundary optimization with SIMSOPT to reduce high-frequency gap spectral content (while maintaining QS, aspect ratio):

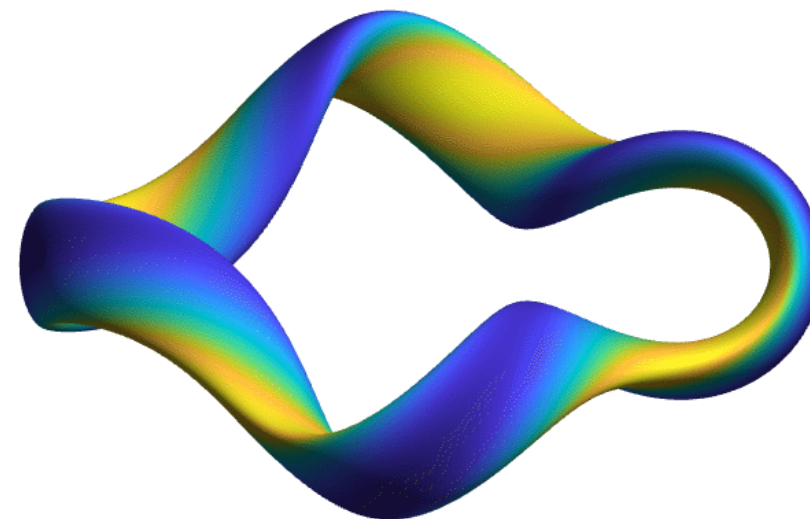
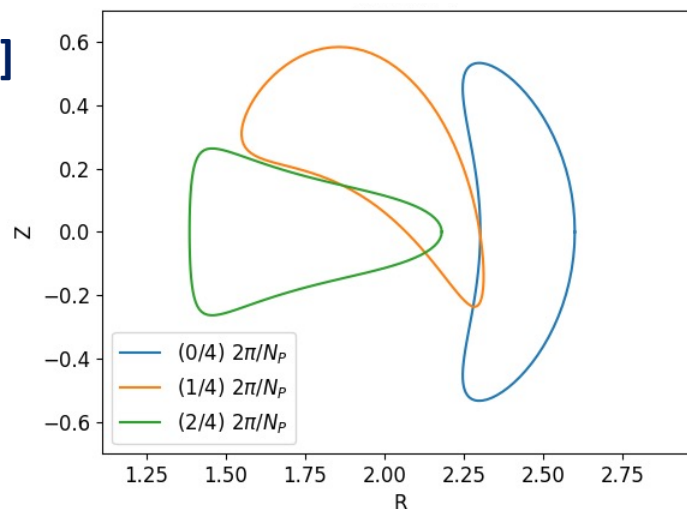
$$f(S_P) = (A(S_P) - A^*)^2 + f_{QS}(S_P) + f_l(S_P) + f_{\text{cont}}(S_P)$$

- f_{QS} : two-term quasisymmetry error
- f_l : enforce $\iota \geq 1.03$
- $f_{\text{cont}} = \sum_s \sum_{\underbrace{|\iota \delta m - N_P \delta n| > |\iota - N|}_{\text{Resonance condition}}} \underbrace{|\epsilon_{\delta m, \delta n}|^2 (\iota \delta m - N_P \delta n)^2}_{\propto (\text{Gap width})^2}$

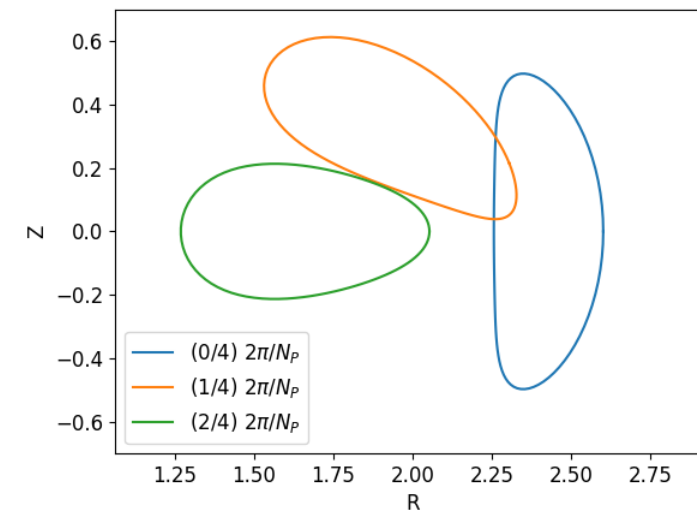
- High-order shaping components reduced



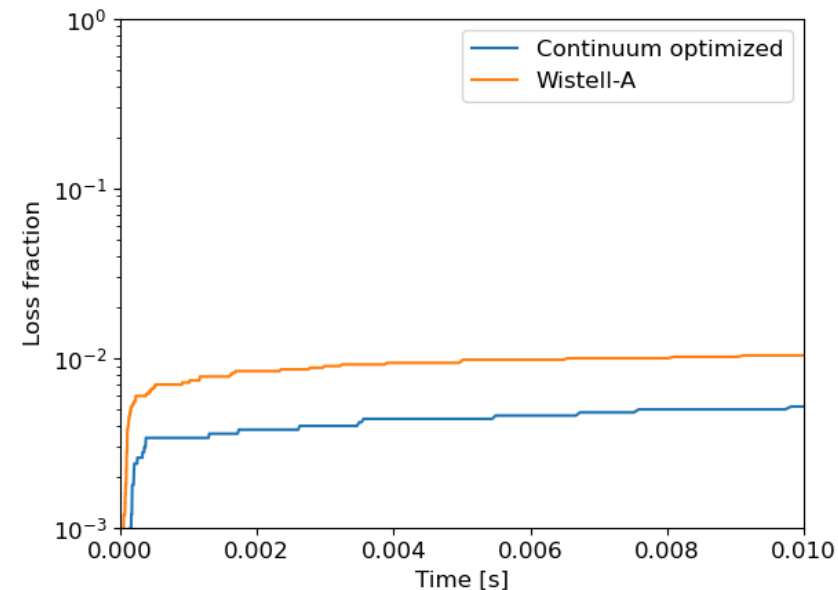
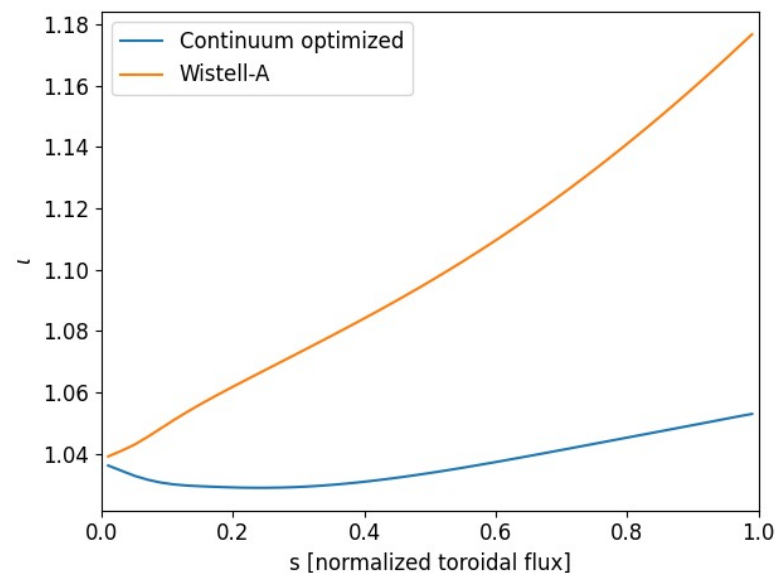
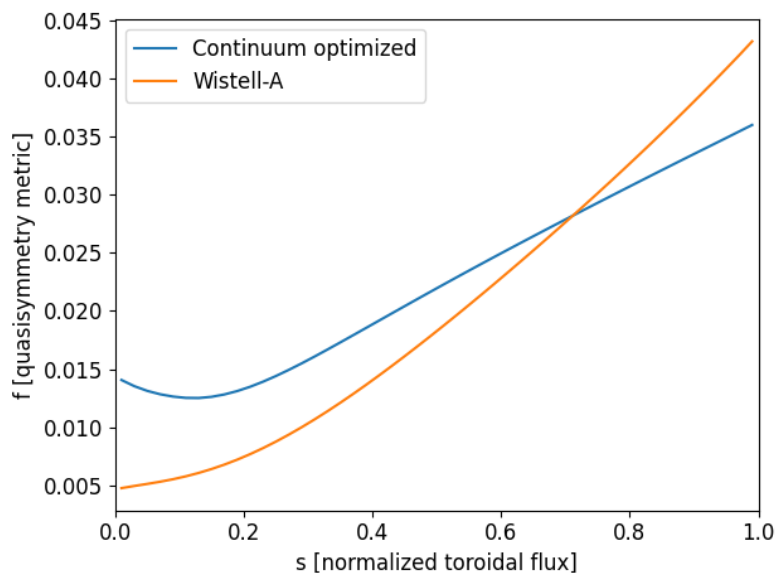
Wistell-A [Bader, 2020]



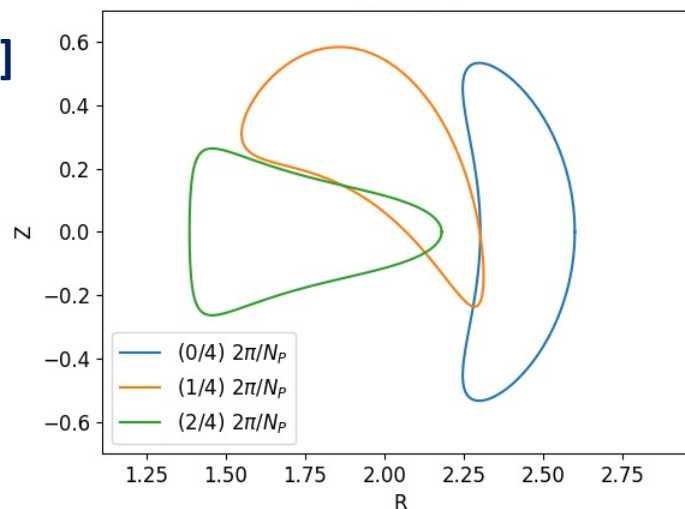
Optimized



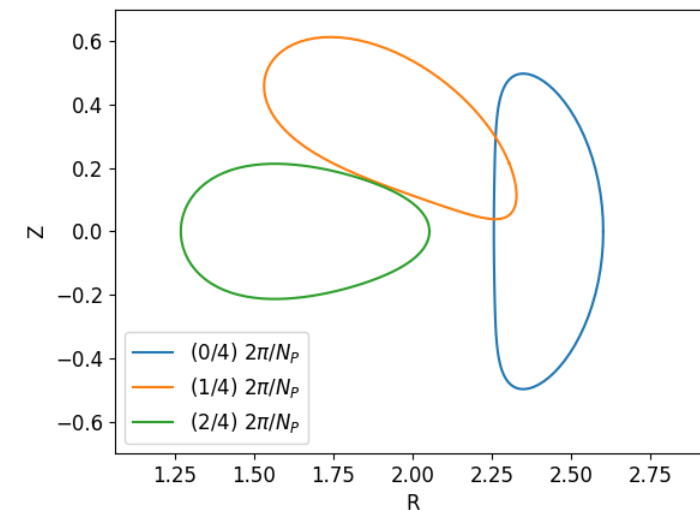
- EP confinement (without MHD activity) maintained



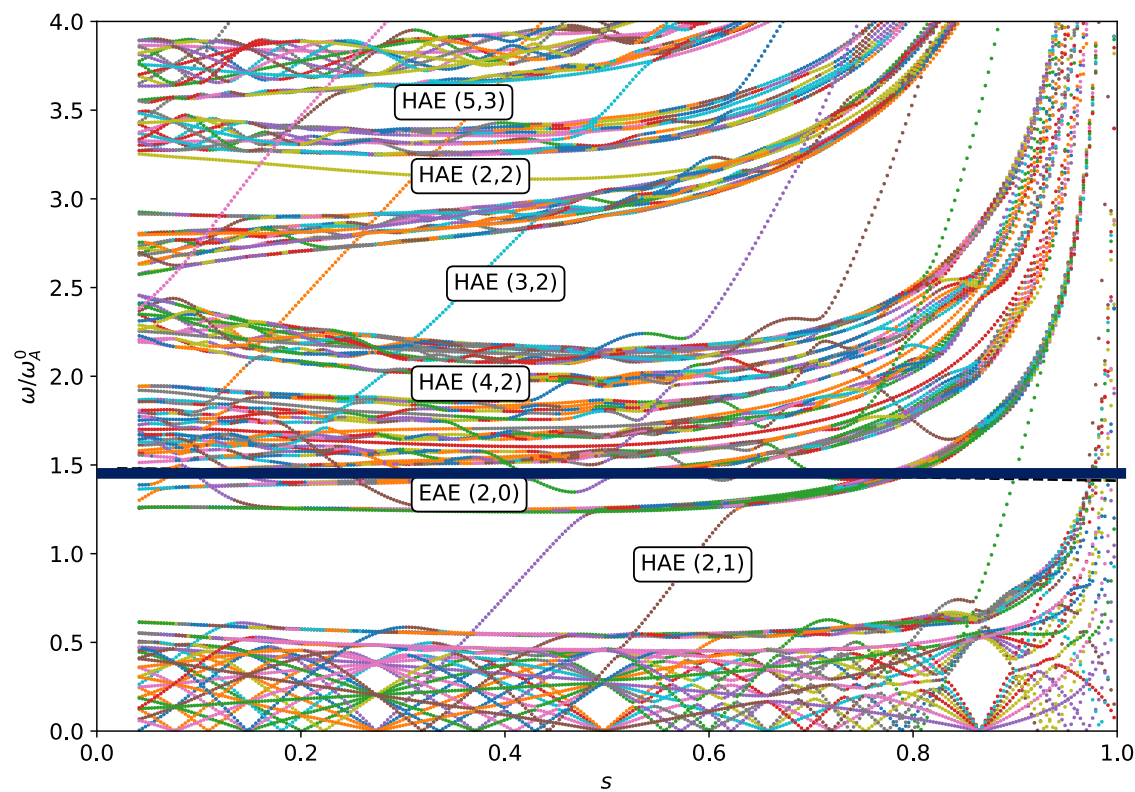
Wistell-A [Bader, 2020]



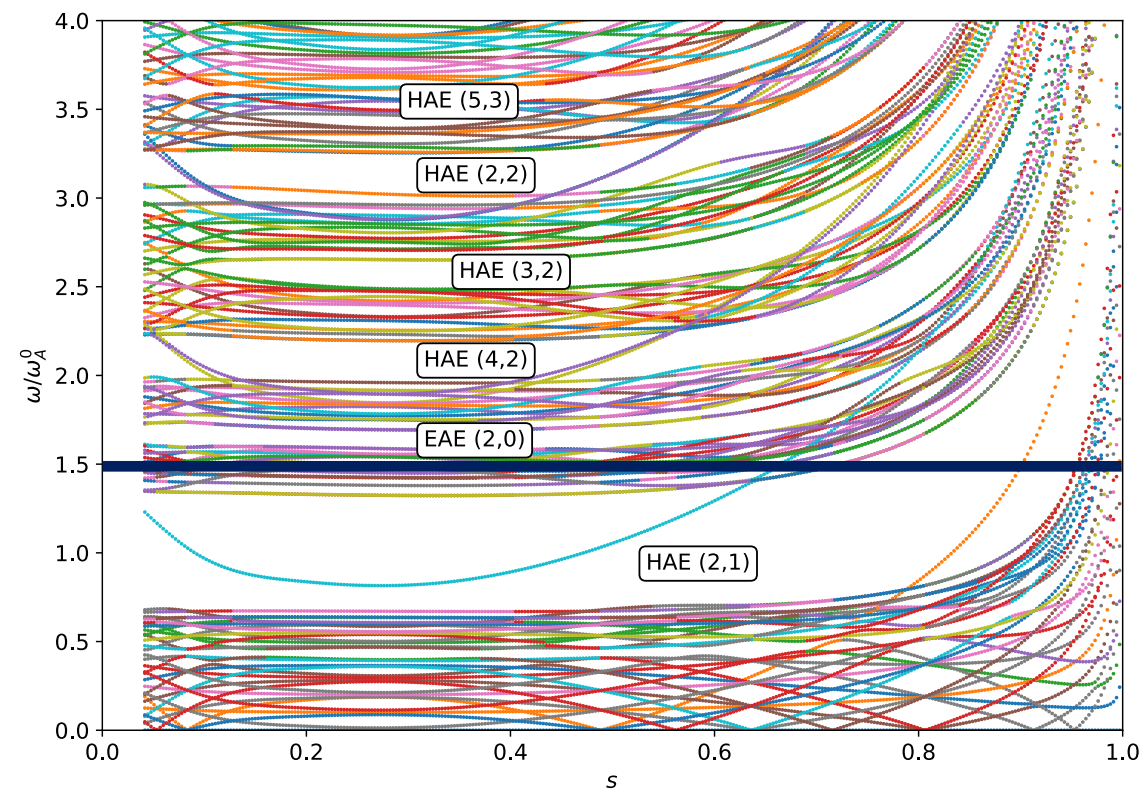
Optimized



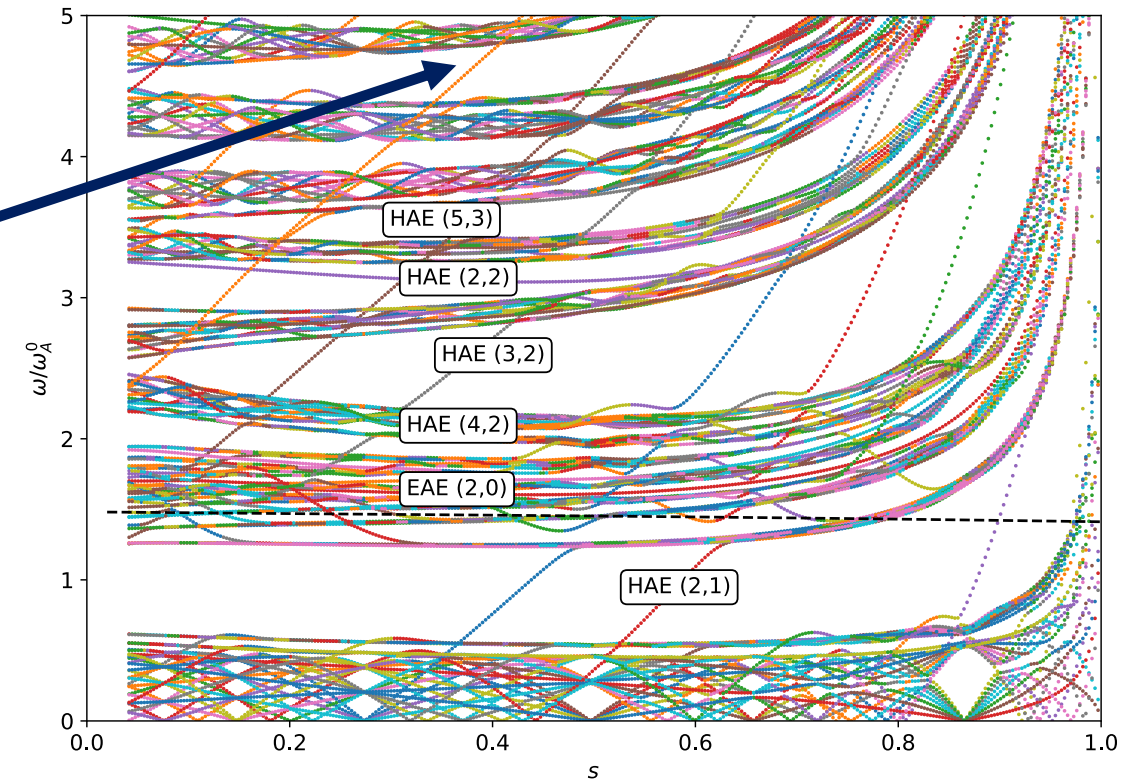
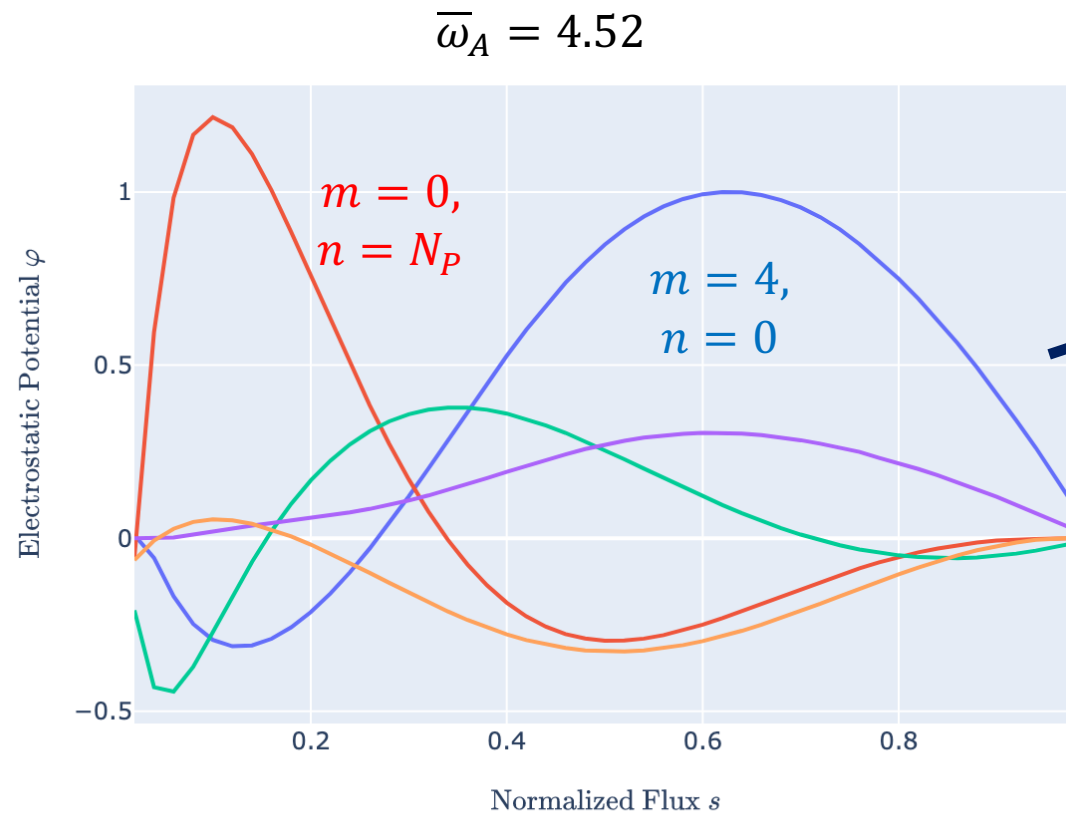
- Stellgap calculations confirm width of high-frequency HAE gaps reduced



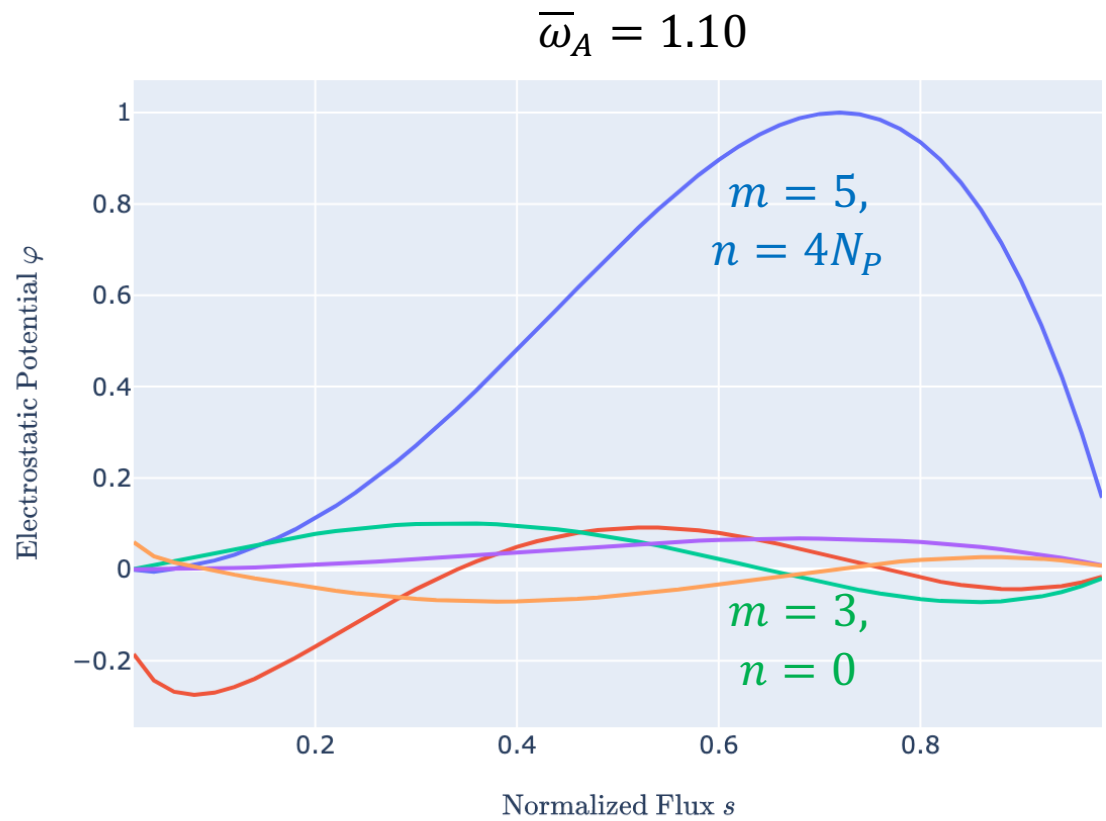
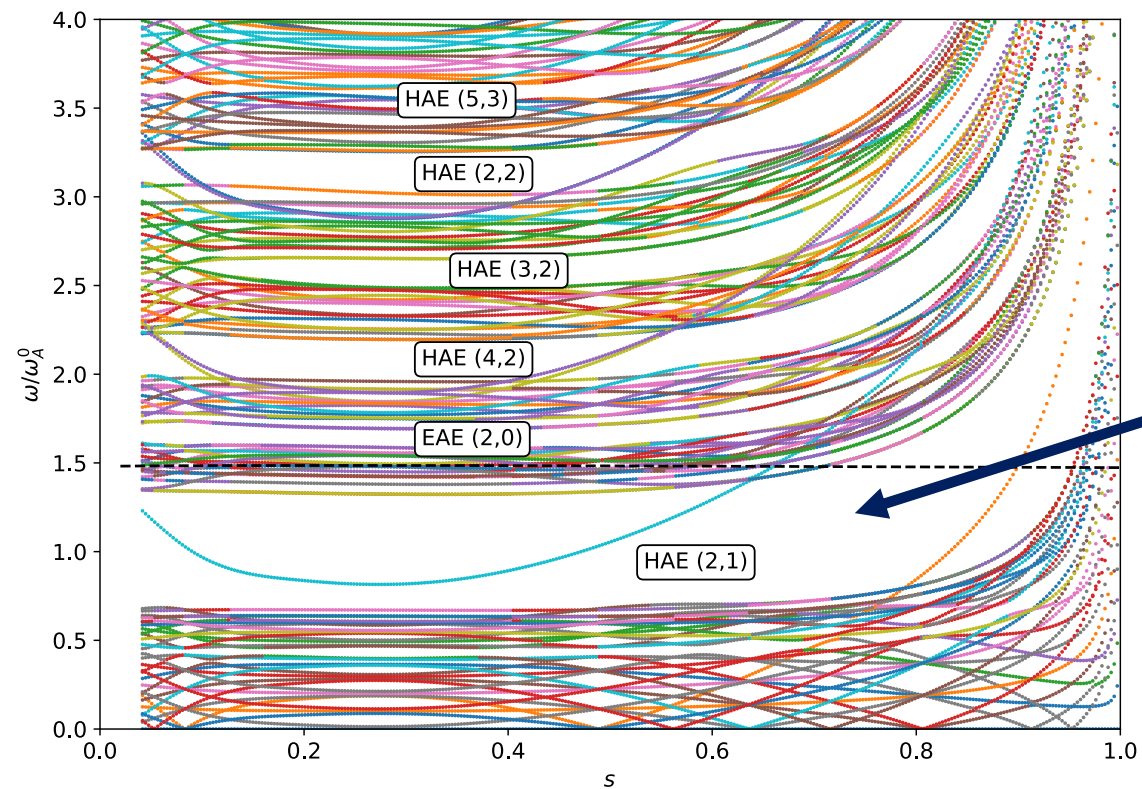
Wistell-A



Optimized

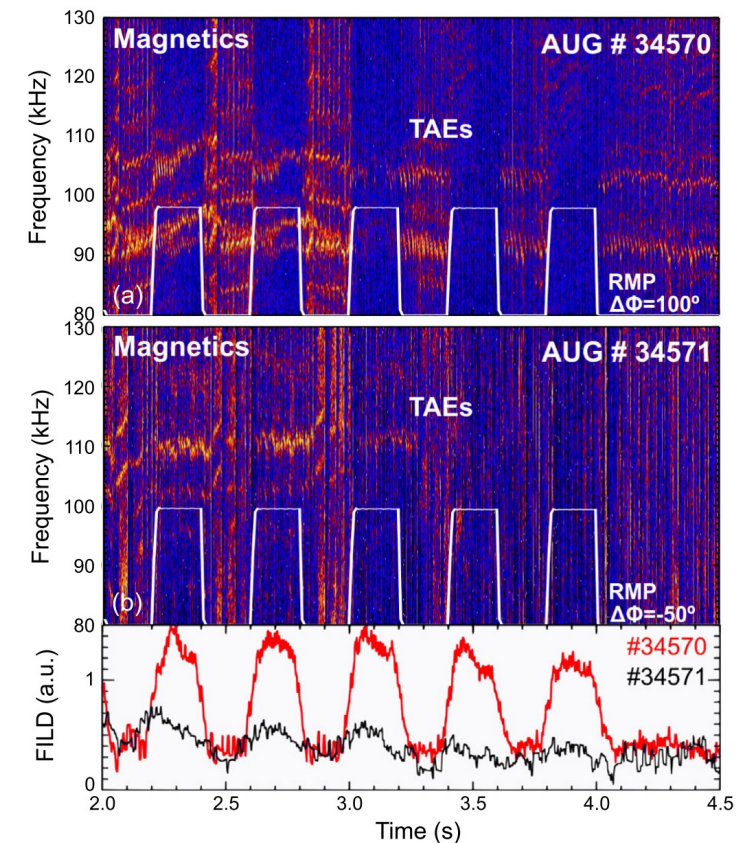


Wistell-A



Optimized

- Geometry can manipulate the continuum to promote stability, by reducing the width of high-frequency gaps which may strongly resonate with EPs
 - Application: control of AEs in tokamaks?



- Geometry can manipulate the continuum to promote stability, by reducing the width of high-frequency gaps which may strongly resonate with EPs
 - Application: control of AEs in tokamaks?
 - Ongoing work: validation of optimization with FAR3D stability analysis
 - Future work: generalization of optimization approach to use spectral density [Weisse, 2006] with full continuum

